MRGPRX4 is a novel bile acid receptor in cholestatic itch

Huasheng Yu[1,2,3], Tianjun Zhao[1,2,3], Simin Liu[1], Qinxue Wu[4], Omar Johnson[4], Zhaofa Wu[1,2], Zihao Zhuang[1], Yaocheng Shi[5], Renxi He[1,2], Yong Yang[6], Jianjun Sun[7], Xiaoqun Wang[8], Haifeng Xu[9], Zheng Zeng[10], Xiaoguang Lei[3,5], Wenqin Luo[4*], Yulong Li[1,2,3*]

[1]State Key Laboratory of Membrane Biology, Peking University School of Life Sciences, Beijing 100871, China

[2]PKU-IDG/McGovern Institute for Brain Research, Beijing 100871, China

[3]Peking-Tsinghua Center for Life Sciences, Beijing 100871, China

[4]Department of Neuroscience, Perelman School of Medicine, University of Pennsylvania, Philadelphia, PA 19104, USA

[5]Department of Chemical Biology, College of Chemistry and Molecular Engineering, Peking University, Beijing 100871, China

[6]Department of Dermatology, Peking University First Hospital, Beijing Key Laboratory of Molecular Diagnosis on Dermatoses, Beijing 100034, China

[7]Department of Neurosurgery, Peking University Third Hospital, Peking University, Beijing, 100191, China

[8]State Key Laboratory of Brain and Cognitive Science, CAS Center for Excellence in Brain Science and Intelligence Technology (Shanghai), Institute of Biophysics, Chinese Academy of Sciences, Beijing, 100101, China

[9]Department of Liver Surgery, Peking Union Medical College Hospital, Chinese

Academy of Medical Sciences and Peking Union Medical College, Beijing 100730, China

[10]Department of Infectious Diseases, Peking University First Hospital, Beijing 100034, China

*Manuscript correspondence:

Yulong Li (yulongli@pku.edu.cn) & Wenqin Luo (luow@pennmedicine.upenn.edu)

Acknowledgments: We thank Dr. Y. Rao for sharing the tissue culture room, Dr. J.H. Zhao for collecting clinical blood samples. We are grateful to Dr. L.Q. Luo and Dr. Y. Song for critical reading of the manuscript. We also thank Dr. X.Z. Dong for sharing unpublished data. This work was supported by the Junior Thousand Talents Program of China to Y.L.

Abstract:

Patients with liver diseases often suffer from chronic itch or pruritus, yet the itch-causing pruritogen(s) and their cognate receptor(s) remain largely elusive. Using transcriptomics and GPCR activation assays, we found that an orphan, primate specific MRGPRX4 is expressed in human dorsal root ganglia (hDRG) and selectively activated by bile acids. *In situ* hybridization and immunohistochemistry revealed that MRGPRX4 is expressed in ~7% of hDRG neurons and co-localizes with HRH1, a known itch-inducing GPCR. Bile acids elicited a robust Ca^{2+} response in a subset of cultured hDRG neurons, and intradermal injection of bile acids and an MRGPRX4 specific agonist induced significant itch in healthy human subjects. Surprisingly, application of agonist for TGR5, a known sequence conserved bile acid receptor previously implicated in cholestatic itch, failed to elicit Ca^{2+} response in cultured hDRG neurons, nor did it induce pruritus in human subjects. *In situ* hybridization and immunostaining results revealed that hTGR5 is selectively expressed in satellite glial cells, unlike mTGR5 (in mouse DRG neurons), likely accounting for the inter-species difference functionally. Finally, we found that patients with cholestatic itch have significantly higher plasma bile acid levels compared to non-itchy patients and the bile acid levels significantly decreased after itch relief. This elevated bile acid level in itchy patients is sufficient to activate MRGPRX4. Taken together, our data strongly suggest that MRGPRX4 is a novel bile acid receptor that likely underlies cholestatic itch, providing a promising new drug target for anti-itch therapies.

INTRODUCTION

Chronic itch, or pruritus, is a severe and potentially debilitating clinical feature associated with many dermatological and systemic conditions[1], severely affecting quality of life and potentially leading to lassitude, fatigue, and even depression and suicidal tendencies[2]. The most well-characterized itch receptors are the H1 and H4 histamine receptors (HRH1 and HRH4)[3]. Although antihistamines, which act by inhibiting histamine receptors, are generally effective at relieving itch symptoms induced by inflammation and allergens, these compounds are usually ineffective at treating chronic itch caused by systemic diseases and most skin disorders. To date, no effective treatment is available for treating histamine-resistant itch[2].

A high percentage of patients with systemic liver failure develop itch with cholestatic symptoms[4]. For example, the prevalence of itch is as high as 69% among patients with primary biliary cirrhosis, and severe itch is an indication for liver transplantation[5]. Moreover, itch occurs in more than half of pregnant woman with intrahepatic cholestasis of pregnancy, a condition that has been associated with an increased risk of preterm delivery, perinatal mortality, and fetal distress[6].

Several medications have been tested for treating cholestatic itch, including ursodeoxycholic acid (UDCA), cholestyramine, and rifampicin; however, these compounds either are ineffective or induce severe side effects[5]. Therefore, safe and effective treatments for cholestatic itch are urgently needed, and identifying the underlying molecular mechanisms—particularly the receptor and ligand—is the essential first step.

Although the link between cholestasis and itch was first described more than

2000 years ago[7], the detailed mechanisms underlying cholestatic itch remain unidentified. To date, a handful of molecules have been proposed as the pruritogens that mediate cholestatic itch, including bile acids, bilirubin, lysophosphatidic acid, autotaxin, and endogenous opioids[4]. With respect to the cognate receptor for the pruritogen, a few receptors have been proposed, albeit based primarily on rodent models. For example, the membrane-bound bile acid receptor TGR5 has been reported to mediate bile acid□induced itch in mice[8,9]. However, a recent study found that administering TGR5-selective agonists failed to elicit an itch response in mouse models of cholestasis[10], raising doubts regarding whether TGR5 is indeed the principal mediator for cholestatic itch. Recently, Meixiong et al. reported that Mrgpra1 and MRGPRX4 (in mice and humans, respectively) can be activated by bilirubin, a compound that serves as one of the pruritogens in cholestatic itch in mice[11]. Nevertheless, the precise molecular mechanism that underlie cholestatic itch in humans remains to be determined.

We specifically focused our search on genes that are selectively expressed in the human dorsal root ganglia (DRG), where the cell bodies of primary itch-sensing neurons are located. Our search revealed a novel ligand-receptor pair comprised of bile acids (the ligand) and the receptor MRGPRX4. Moreover, we found that MRGPRX4 is expressed selectively in a small subset of neurons in the human DRG, and bile acids directly trigger intracellular Ca^{2+} increase in these neurons. In addition, intradermal injection of both bile acids and the MRGPRX4-specific agonist nateglinide induce detectable itch in human subjects, and this bile acid-induced itch is

histamine-independent. Surprisingly, application of agonist for TGR5, a known sequence conserved bile acid receptor previously implicated in cholestatic itch, failed to elicit Ca^{2+} response in cultured hDRG neurons, nor did it induce pruritus in human subjects. In situ hybridization and immunostaining results revealed that unlike mTGR5 expressing in mouse DRG neurons, hTGR5 is selectively expressed in satellite glial cells, likely accounting for the inter-species difference functionally. Finally, we found that plasma bile acid levels are well correlated with itch sensation in cholestatic patients and that this elevated bile acid level is sufficient to activate MRGPRX4. Taken together, our results provide compelling evidence that the ligand-receptor pair of bile acids and MRGPRX4 is likely to be one of the critical mediators for human cholestatic itch.

RESULTS

MRGPRX4 is activated by bile extract

DRG neurons are primary somatosensory neurons that express a variety of receptors and ion channels for detecting both extrinsic and intrinsic stimuli[12]. To identify a receptor in mediating cholestatic itch in human, we reason that this candidate receptor could be expressed in human DRG neurons and activated by bile extracts. Since the majority of itch receptors identified to date belong to the G protein□coupled receptor (GPCR) superfamily[13], we analyzed two published transcriptomics datasets compiled from a variety of human tissues[14,15], specifically focusing on GPCRs. Among the 332 transcripts that are enriched in the human DRG (Table S1), we

identified the following seven highest-enriched orphan GPCRs: GPR149, MRGPRX4, GPR139, GPR83, MRGPRE, MRGPRX1, and MRGPRD[16,17] (**Fig. 1a and Table S2**). Next, we cloned and expressed these candidate receptors in HEK293T cells (**Supplementary Fig. 1a, b**), finding that all seven receptors were expressed at the plasma membrane (**Supplementary Fig. 1b**). We measured the activation of each receptor by bovine bile extract using two reporter assays, the Gs-dependent luciferase assay[18] and the Gq-dependent TGFα shedding assay[19] (**Fig. 1b,c**). No signal was detected with the Gs-dependent luciferase assay (**Fig. 1b**). Interestingly, bile extract elicited a significant increase in reporter activity in cells expressing MRGPRX4 measured using the TGFα shedding assay, but had no effect on cells expressing the other six GPCRs (**Fig. 1c**). These results suggest that MRGPRX4 is activated by one or more compounds present in bile extract, and that MRGPRX4 likely signals through the Gq but not the Gs pathway. Further experiments revealed that bovine, porcine, and human bile extract activate MRGPRX4 to a similar extent in a dose-dependent manner (**Fig. 1d**); in contrast, extracts obtained from bovine brain, spleen, heart, kidney, and liver tissues induced no detectable signal on MRGPRX4-expressing cells (**Fig. 1e**). Taken together, these results suggest that MRGPRX4 is potently activated by bile extract and active compound(s) is/are highly enriched in bile extract.

Identifying which in bile extract activate MRGPRX4

Next, to identify the component(s) in bovine bile extract that activate(s) MRGPRX4,

we separated the extract into six fractions using silica gel column chromatography (**Fig. 2a**). Each fraction was then applied to MRGPRX4-expressing HEK293T cells, and MRGPRX4 activation was measured using the TGFα shedding assay. Among the six fractions tested, fraction 4 caused the strongest activation of MRGPRX4, whereas fractions 1 and 6 caused the weakest activity (**Fig. 2b**), indicating that the active component(s) are mainly present in fraction 4. Mass spectrometry of fractions 4 and 6 revealed a peak enriched specifically in fraction 4 (**Fig. 2c**); this peak corresponded to ions with an m/z value of 410.3265 in the positive ion mode and was annotated to prostaglandin F2α diethyl amide and/or dihydroxy bile acids. Further experiments using ^{1}H-NMR revealed that two pure dihydroxy bile acids—deoxycholic acid (DCA) and chenodeoxycholic acid (CDCA)—produced peaks that were identical to the peaks in fraction 4 (**Fig. 2d**); other fractions that only weakly activated MRGPRX4 also contained characteristic peaks of bile acids as shown by ^{1}H-NMR (**Supplementary Fig. 2**). These results suggest that DCA and/or CDCA are enriched in the active fraction of bile extract and may be the key compounds that activate MRGPRX4.

Characterization of bile acids: MRGPRX4 activation and the downstream signaling

To further characterize the efficacy and potency of DCA, CDCA, other bile acids, and their derivatives in activating MRGPRX4, we systematically measured their ability to activate MRGPRX4 in HEK293T cells, using TGFα shedding assay and FLIPR

(fluorescent imaging plate reader) Ca^{2+} assay. All of the bile acids tested activated MRGPRX4 to some extent; DCA had the highest potency measured with both assays, with an EC_{50} value of 2.7 μM and 2.6 μM in the TGFα shedding and FLIPR assays, respectively; cholic acid (CA), CDCA, and lithocholic acid (LCA)—three close analogs of DCA—were less potent (**Fig. 3a-c**). Based on the structural differences between DCA and the less potent bile acids, we reasoned that hydroxylation at position of R1 and/or R2, as well as taurine/glycine conjugation at position R3, is important for specific bile acids to activate MRGPRX4 (**Fig. 3c**).

Next, we examined the potential signaling events downstream of bile acid-induced MRGPRX4 activation by measuring intracellular Ca^{2+} concentration ($[Ca^{2+}]_i$) in MRGPRX4-expressing HEK293T cells loaded with Fluo-8 AM, a fluorescent Ca^{2+} indicator. We found that DCA, CA, CDCA, and LCA induced a robust fluorescence response in these cells (**Fig. 3d-f**), and pretreating the cells with the phospholipase C inhibitor U73122 significantly reduced the DCA-evoked Ca^{2+} signals; in contrast, the Gβγ inhibitor gallein had no effect on DCA-evoked signaling (**Fig. 3g-h**). Taken together, these results indicate that a Gq-dependent signaling pathway involving phospholipase C is downstream to MRGPRX4 activation by bile acids.

Interestingly, even though MRGPRX1, MRGPRX2, and MRGPRX3 are close analogs of MRGPRX4, none of these receptors was activated by bile acids, even at 100 μM concentration (**Supplementary Fig. 3a-e**). We therefore investigated the putative ligand-binding sites in MRGPRX4 by comparing the primary amino acid sequence of MRGPRX4 with these three analogs (**Fig. 3i**). We identified amino acid

198 residues that are conserved in MRGPRX1, MRGPRX2, and MRGPRX3 but not in
199 MRGPRX4 and mutated these residues, once per time, to an alanine residue in
200 MRGPRX4. We found that mutating amino acids 159, 180, and 235 reduced the
201 receptor's affinity for DCA (**Fig. 3j**), without affecting trafficking to the cell membrane
202 (**Fig. 3k**); thus, these three sites may play a critical role in the binding of bile acids to
203 MRGPRX4. In addition, we examined whether mouse and/or rat Mrgpr family
204 members also respond to bile acids. Intriguingly, bile acids failed to activate any
205 mouse or rat Mrgpr members tested (**Supplementary Fig. 3g-h**), suggesting that the
206 ability of MRGPRX4 to sense bile acids may be a new functional addition during
207 evolution.
208
209 ***A subset of human itch-related DRG neurons express MRGPRX4 and respond***
210 ***to bile acids***
211 Next, we examined endogenous expression pattern of MRGPRX4 in hDRGs. We
212 performed *in situ* hybridization using a digoxigenin-labeled riboprobe against
213 *MRGPRX4* mRNA, and found that *MRGPRX4* mRNA is expressed in only ~6-8% of
214 hDRG neurons (**Fig. 4a, c**); similar results were obtained with immunofluorescence
215 using an MRGPRX4-specific antibody (**Fig. 4b, c** and **Supplementary Fig. 4**).
216 Morphologically, these MRGPRX4-expressing neurons are small-diameter neurons,
217 with a diameter of approximately 50 μm, which is similar to small-diameter neurons
218 that express the neurotrophic tyrosine kinase receptor type 1 (TrkA) (**Fig. 4d**),
219 suggesting a function in nociception and/or pruriception[20].

To further characterize the molecular profile of these MRGPRX4-positive hDRG neurons, we performed triple-labeling of MRGPRX4 and two additional molecular markers using RNAscope *in situ* hybridization (**Fig. 4e**). Our analysis revealed that >90% of MRGPRX4-positive neurons also express the histamine receptor HRH1, a well-characterized itch receptor in humans[21], and TRPV1 (transient receptor potential cation channel subfamily V member 1) (**Fig. 4f-g**), which functions downstream of Mrgprs and histamine receptors[22,23]. Interestingly, the majority of MRGPRX4-expressing neurons also co-express $Na_v1.7$ voltage-gated sodium channel, the peptidergic marker CGRP (calcitonin gene-related peptide), and TrkA[24,25] (**Fig. 4f-g**). These results suggest that MRGPRX4 is specifically expressed in a subset of small diameter peptidergic hDRG neurons.

Next, we tested whether MRGPRX4 in DRG neurons can be activated by bile acids. Because bile acids failed to induce a detectable Ca^{2+} signal in cultured rat DRG neurons (**Supplementary Fig. 5**), we expressed the human MRGPRX4 in cultured rat DRG neurons. Bile acids triggered a robust Ca^{2+} response in MRGPRX4-expressing rat DRG neurons (**Supplementary Fig. 5**), indicating that MRGPRX4 expressed in rat DRG neurons mediates the bile acid induced activation. Consistent with our finding that DCA is a more potent agonist of MRGPRX4 than CA, DCA induced a significantly larger Ca^{2+} response and activated a larger number of MRGPRX4-expressing rat DRG neurons than CA (**Supplementary Fig. 5**).

Next, we asked whether hDRG neurons can also be activated by bile acids. Application of DCA induced a robust fluorescence increase in a subset (~6%) of these

hDRG neurons loaded with Fluo-8 AM; this percentage of DCA-responsive cells is similar to the percentage of MRGPRX4-expressing cells measured with *in situ* hybridization (**Fig. 4a, c**). Moreover, the less potent MRGPRX4 agonist CA also induced a response, albeit much weaker than DCA (**Fig. 4h** and **Supplementary Fig. 6**). In addition, nearly all (~90%) of DCA-responsive hDRG neurons were capsaicin-sensitive, and approximately one-third of DCA-responsive neurons also responded to histamine (**Fig. 4j**). Together, our results indicate that expression of MRGPRX4 is sufficient to render bile acid sensitivity of primary somatosensory neurons.

Pharmacological activation of MRGPRX4 triggers itch sensation in human subjects

Given the specific expression pattern of MRGPRX4 in a subset of hDRG neurons, and the known role of Mrgpr family members in mediating itch sensation, we next asked whether pharmacologically activating MRGPRX4 could trigger itch sensation in human subjects. We recruited healthy volunteers and performed a double-blind skin itch test, in which each subject received a 25-μl intradermal injection of the test compounds or vehicle in four separate sites on both forearms (**Fig. 5a1, inset**), after which the subject was asked to rank the itch sensation at each injection site using a generalized labeled magnitude scale (LMS)[26]. Interestingly, the pharmacological MRGPRX4 specific agonist nateglinide, a previously reported MRGPRX4 agonist[27], (**Supplementary Fig. 3f**) —but not vehicle—induced a robust itch sensation in

healthy subjects (**Fig. 5a1, a2**). These results show that activation of MRGPRX4 is sufficient to trigger itch sensation in humans, suggesting that MRGPRX4 is a human itch receptor.

Bile acid-induced itch in humans is both histamine- and TGR5-independent

Previous studies have implicated that bile acids could induce itch in human[28,29]. Here, we systematically test pruritic effect of bile acids on human and whether bile aicd-induced itch shows some features similar to that of cholestatic itch[17]. We found that 500 μg (25 μl) of DCA induced a significant itch sensation that peaked within 5 min and declined slowly over time; in contrast, control injections with vehicle did not induce an itch response (**Fig. 5a1, a2**). Moreover, itch intensity induced by DCA was in a dose-dependent manner (**Fig. 5b1, b2**). We also found that less potent MRGPRX4 agonists, including CA, CDCA, taurochenodeoxycholic acid (TCDCA), and LCA, also induced a weaker—albeit still significant—itch sensation (**Fig. 5c1, c2**). Given that antihistamines are largely ineffective for treating cholestatic itch[4], we tested whether itch induced by bile acids can be blocked by antihistamines. We found that pretreating subjects with an antihistamine prevented histamine-induced itch but had no effect on DCA-induced itch (**Fig. 5d1, d2**), suggesting that itch induced by bile acids does not involve histamine signaling. Taken together, these results indicate that bile acids trigger an itch sensation with features similar to cholestatic itch.

In mice, the membrane bile acid receptor TGR5 has been reported to mediate bile acid-induced itch[8,9]. To test whether bile acid-induced itch in human is also

mediated by TGR5, we chose a non-bile acid TGR5 agonist compound 15[30], which is nearly 70-fold more potent than DCA in activating human TGR5 and does not activate human MRGPRX4 (**Fig. 6b, c**). Intradermal injections of 10 μg (25μl) of compound 15 did not induce detectable itch in humans, whereas DCA, as the positive control, induced significant itch (**Fig. 6a1, a2, d**). These results suggest that TRG5 is not the receptor mediating bile acid-induced itch. Furthermore, we examined the expression of TGR5 in the human, monkey, and mouse DRG tissues. Very surprisingly, although the amino acid sequence of TGR5 is relatively conserved between rodents and primates (**Supplementary Fig. 7a**), we found the different expression pattern of TGR5 in DRG tissues. In human and monkey, both *in situ* hybridization and immunostaining revealed that TGR5 is highly expressed in satellite glial cells surrounding DRG neurons but not the primary sensory neurons (**Fig. 6e-i and Supplementary Fig. 7**), while in mouse, the same *in situ* probe and antibody detected the expression of TGR5 in mouse DRG neurons (**Fig. 6f, h and Supplementary Fig. 7c**), similar to the previous publication[8,9]. These results revealed an interesting species difference in TGR5 expression and function between mouse and primate. Taken together, our results demonstrate that the function of TGR5 in human somatosensory system is different from that in mouse, and TGR5 is not the receptor for mediating bile acid-induced itch in human.

The elevated levels of bile acids in cholestatic itchy patients are sufficient to activate MRGPRX4

Lastly, to investigate whether bile acids are the pruritogens under pathological conditions, we collected plasma samples from patients with liver or skin diseases and measured the concentration of 12 major bile acids using HPLC-MS/MS (**Fig. 7a and Supplementary Fig. 8a**). We found that glycine- and taurine-conjugated primary bile acids, including glycocholic acid (GCA), taurocholic acid (TCA), glycochenodeoxycholic acid (GCDCA), and TCDCA are the major bile acids present in cholestatic patients (**Fig. 7a**), consistent with previously published results[31-33]. Compared to itchy patients with liver diseases, non-itchy patients had significantly higher levels of total bile acids (defined here as the sum of the 12 bile acids shown in **Fig. 7a**) (**Fig. 7a, b**). The level of total plasma bile acids in the itchy patients with skin diseases was barely detectable and significantly lower than the itchy patients with liver diseases. Among the 12 bile acids measured, the ones with the largest differences between the patients with itch and those without itch were for GCA, GCDCA, TCA, and TCDCA (**Fig. 7a, b**), suggesting that these four bile acids play key roles in mediating chronic itch under pathological conditions. Indeed, intradermal injections of TCDCA caused significant itch in healthy subjects (**Fig. 5c1, c2**). For DCA, the most potent ligand for MRGPRX4 among all tested bile acids, we did not see the significant difference between itchy and non-itchy patients with liver diseases (**Fig. 7a**), suggesting it is not the major contributor for cholestatic itch under pathological conditions. More importantly, although bile acid levels vary among itchy patients with liver diseases both from our data (**Fig. 7a, b**) and previously reported results[32-34], we found that the total plasma bile acids, as well as the individual levels of

GCDCA, TCDCA, TCA, and GCA, significantly decreased in 11 out of 13 patients following itch relief (**Fig. 7c, d** and **Supplementary Fig. 8c**). Taken together, these results suggest that high levels of bile acids are well correlated with itchy symptom in patients with liver diseases and that bile acids—particularly GCDCA, TCDCA, TCA, and GCA— could be main metabolites triggering cholestatic itch.

Next, we examined whether combinations of bile acids at pathologically relevant levels are sufficient to activate MRGPRX4. We prepared mixtures of bile acids similar to the plasma/serum levels in healthy subjects ("healthy mix") or in patients with liver diseases and itch ("liver itch mix"), which are estimated based on previously published data[31,35] and our quantification results (**Fig. 7a**). These mixtures were then applied to MRGPRX4-expressing HEK293T cells while performing Ca^{2+} imaging. We found that the "liver itch mix" but not "healthy mix" induced a significant Ca^{2+} signal (**Fig. 7e, f**), suggesting that pathological relevant level of bile acids is sufficient to activate MRGPRX4.

Recently, Meixiong et al. reported that MRGPRX4 can also be activated by bilirubin, which is another potential pruritogen for triggering cholestatic itch[11]. We therefore compared bilirubin and DCA with respect to binding and activating MRGPRX4. We found that compared to bile acids, bilirubin is a less potent, partial agonist of MRGPRX4 (**Supplementary Fig. 9a**). Given the structural differences between bilirubin and DCA, we then tested whether bilirubin is an allosteric modulator of MRGPRX4. Indeed, we found that bilirubin can potentiate the activation of MRGPRX4 by DCA (**Supplementary Fig. 9b**), and—conversely—DCA potentiate the

activation of MRGPRX4 by bilirubin (**Supplementary Fig. 9c**). Moreover, we found that both total bilirubin and conjugated bilirubin levels were significantly higher in itchy patients with liver diseases compared to non-itchy patients (**Supplementary Fig. 9d**) and plasma bilirubin levels decreased significantly after itch relief (**Supplementary Fig. 9e**). Compare to total bilirubin, total bile acids show better correlation with itch intensity (measured using a self-report numerical rating scale[36]) (**Supplementary Fig. 9f**). Taken together, these results suggest that bile acids are the major pruritogens in MRGPRX4-mediated cholestatic itch and bilirubin facilitates the activation of MRGPRX4 by bile acids and may also contribute to cholestatic itch in pathological conditions.

DISCUSSION

Here, we report that MRGPRX4 is a novel GPCR that fits with the criteria we set for identifying putative receptor in mediating cholestatic itch. MRGPRX4 is selectively expressed in a small subset of human DRG neurons. Bile acids triggered a robust Ca^{2+} response in a subset of hDRG neurons as well as rat DRG neurons expressing MRGPRX4 exogenously. Both bile acids and an MRGPRX4-specific agonist induce itch in human. Bile acid-induced itch in human is histamine independent, which is consistent with antihistamines are largely ineffective for treating cholestatic itch. Surprisingly, application of agonist for TGR5 failed to elicit Ca^{2+} response in cultured hDRG neurons, nor did it induce pruritus in human subjects. The expression pattern of TGR5 is different between mouse and human. hTGR5 is selectively expressed in

satellite glial cells, while mTGR5 is expressed in DRG neurons, likely accounting for the inter-species difference functionally. We also found that plasma levels of bile acids were well correlated with itchy patients with liver diseases. Importantly, a mixture of bile acids with components and concentrations similar to that of cholestatic itchy patients—but not healthy volunteers—was sufficient to activate MRGPRX4. Our data indicate bile acids are the major pruritogens in MRGPRX4-mediated cholestatic itch and bilirubin facilitates the activation of MRGPRX4 by bile acids and may also contribute to cholestatic itch in pathological conditions. Based on our results, we propose a new working model for cholestatic itch (**Fig. 7g**): patients with cholestasis usually display increased plasma levels of bile acids and bilirubin, which are precipitated in the skin and activate MRGPRX4 receptors in itch-related primary fibers, thereby triggering itch in these patients. Our results exclude TGR5 as a primary itch receptor in human, and the broad expression of TGR5 in satellite glial cells implies a more general function which remains to be determined in the future.

Here, we provide important evidence that MRGPRX4 is sufficient for mediating bile acid□induced itch, and thus should play an important role in cholestatic itch. Since specific antagonist for MRGPRX4 is currently unavailable, we could not determine whether MRGPRX4 is necessary for bile acids induced itch in human. Future studies will be designed to further examine the role of MRGPRX4 in cholestatic itch using to-be-developed pharmacological and/or human genetic approaches. For example, several single-nucleotide polymorphisms (SNPs) have been identified in the human *MRGPRX4* gene[37], and it would be interesting to screen

for loss-of-function and gain-of-function *MRGPRX4* variants. Characterizing the relationship between these variants and itch intensity in cholestatic patients and healthy subjects with bile acid□induced itch could help to further delineate the relationship between MRGPRX4 activity and cholestatic itch. These experiments will also help to determine whether MRGPRX4 is the main molecular receptor for mediating cholestatic itch, or whether other GPCRs[4], such as lysophosphatidic acid receptors and serotonin receptors also play roles in cholestatic itch.

Our current understandings about mechanisms underlying somatosensation in the mammalian system are mainly derived from studies of rodents. Despite the great value and insights we gained using rodent models, notable failures have happened in translating results obtained in rodents into effective and safe clinical treatments in human[38-41]. The bile acid receptors we study here is a great example demonstrating the species differences between rodent and human somatosensory systems. Although TGR5, a bile acid membrane receptor, was previously reported to be expressed in mouse DRG neurons and mediate bile acid□induced itch in mice[8,9], our expressing characterizations as well as functional assays revealed that TGR5 is not expressed in human DRG neurons and doesn't directly mediate itch sensation in human. Instead, primate MRGPRX4 gains the novel function of bile acid sensitivity during evolution. Therefore, it is crucial to study and validate the mechanism of cholestatic chronic itch and develop the correspondent treatment within the context of human physiology.

Recently, Meixiong et al. reported that mouse Mrgpra1 and human MRGPRX4

418 can be activated by bilirubin, suggesting that bilirubin may serve as a pruritogen in
419 cholestatic itch[11]. Bilirubin, a yellow compound that causes the yellow discoloration in
420 jaundice, has not been considered a likely candidate pruritogen though, because the
421 clinical observation that itch often precedes the appearance of jaundice, particularly in
422 patients with intrahepatic cholestasis of pregnancy (ICP)[42] and patients with primary
423 biliary cirrhosis[7]. Our results suggest that bilirubin is a partial agonist of MRGPRX4
424 and may potentiate the activation of MRGPRX4 by bile acids. This notion is
425 consistent with our finding that the correlation between bile acid levels and itch
426 intensity is stronger than the correlation between bilirubin levels and itch intensity.
427 Based on these findings, we propose that bile acid is the major contributor to
428 cholestatic itch, and bilirubin serves to increase bile acid□induced cholestatic itch
429 under pathological conditions.

430 In summary, we found that the membrane-bound GPCR MRGPRX4 is a novel bile
431 acid receptor and may serve as an important molecular mediator of chronic itch in
432 patients with systemic liver diseases. Our results suggest that MRGPRX4 is a
433 promising molecular target for developing new treatments to alleviate devastating
434 chronic itch in these patients.

435

436 **Data availability statement**

437 The data that support the findings of this study are available from the corresponding
438 author upon request. All figures have associated raw data. There is no restriction
439 regarding data availability.

Conflict of interest

The authors declare no competing interests.

Figures and legends

Fig. 1 MRGPRX4 is activated by bile extract.

(**a**) Flow chart for the strategy used to identify orphan GPCRs enriched in human DRG. Transcriptome analysis of DRG and other tissues (trigeminal ganglia, brain, colon, liver, lung, skeletal muscle, and testis) revealed 332 transcripts with high expression in the DRG. The top seven orphan GPCRs are listed. See also Supplementary Tables S1 and S2. Gene expression data were obtained from Flegel et al. *PLoS One*, 2013 & 2015.

(**b** and **c**) Activation of MRGPRX4 by bovine bile extract. The diagrams at the top depict the reporter gene assays used to measure GPCR activation via Gs-dependent (**b**) and Gq-dependent (**c**) pathways. The seven GPCRs identified in (**a**) were tested, revealing that MRGPRX4-expressing HEK293T cells are activated by bile extract via the Gq-dependent pathway. Forskolin and TPA were used as positive controls for activating Gs- and Gq-dependent signaling, respectively. The responses obtained

462 from the tested GPCRs were normalized to the responses induced by respective
463 positive controls. As positive controls for detecting GPCR activation, separate cells
464 were transfected with ADRB1 and stimulated with 10 μM norepinephrine (NE) (**b**) or
465 transfected with HRH1 and stimulated with 10 μM histamine (His) (**c**). "HEK (only)"
466 refers to non-transfected cells. n = 3 experiments performed in triplicate.
467 (**d**) Concentration-response curve for the activation of MRGPRX4 by bovine bile
468 extract, porcine bile extract, and human bile measured using the TGFα shedding
469 assay. The bovine and porcine bile extract solutions were diluted 1 :10 from a 100 μ
470 g/ml stock solution, and the human bile solution was diluted 1:10 from crude human
471 bile. n = 2 experiments performed in triplicate.
472 (**e**) MRGPRX4 is activated selectively by bovine, porcine, and human bile extracts,
473 but not by bovine brain, spleen, heart, kidney, or liver tissue extracts. The data for
474 porcine and human bile are reproduced from (**d**). n = 2 experiments performed in
475 triplicate. Student's *t*-test, **p* < 0.05, ****p* < 0.001, and n.s. not significant (*p* > 0.05).
476
477 **Fig. 2 Identification of the active components in bile extract that activate**
478 **MRGPRX4.**
479 (**a**) Flow chart depicting the strategy for isolating and identifying candidate MRGPRX4
480 ligands in bovine bile extract. F1 through F6 indicate the six fractions used in
481 subsequent experiments.

(**b**) Activation of MRGPRX4 by bile extract fractions F1 through F6; fraction F4 has the highest activity. The data represent one experiment performed in triplicate. Student's *t*-test, $^{**}p < 0.01$. $^{***}p < 0.001$ versus fraction F4.

(**c**) MS analysis of fractions F4 and F6 (which showed high and weak activity, respectively). The selectively enriched peak in fraction F4 at molecular weight 410.3265 corresponds to the bile acids DCA and CDCA.

(**d**) ^{1}H-NMR analysis of fractions F4 and F6 using purified DCA and CDCA as controls.

Fig. 3 Functional characterization and molecular profiling of bile acids as ligands for MRGPRX4.

(**a-c**) Dose-dependent activation of MRGPRX4 by various bile acids and their derivatives. MRGPRX4 activation was measured using the TGFα shedding assay (**a**) or the FLIPR assay (**b**, see methods) in MRGPRX4-expressing HEK293T cells; n = 1 experiment performed in triplicate. The general structure of the bile acids and derivatives is shown in (**a**), and the respective potencies of the bile acids/derivatives are listed in (**c**).

(**d-f**) Activation of MRGPRX4 by various bile acids in cells loaded with the Ca^{2+} indicator Fluo-8 AM. (**d**) Representative images of MRGPRX4-expressing HEK293T cells (shown by mCherry fluorescence) before and after application of 10 μM DCA. (**e**) Representative traces of Ca^{2+} responses induced by application of 10 μM DCA, CA, CDCA, or LCA. n = 50 cells each.

(**g-h**) MRGPRX4 is coupled to the Gq-PLC-Ca^{2+} signaling pathway. DCA (10 μM) evoked a robust Ca^{2+} signal in MRGPRX4-expressing HEK293T cells (**g**, left); this response was blocked by pretreating cells for 30 min with the PLC inhibitor U73122 (**g**, middle), but not the Gβγ inhibitor gallein (**g**, right). Triton X-100 was used as a positive control. The summary data are shown in (**h**); n = 7-10 cells each. Student's *t*-test, ***$p < 0.001$, and n.s. = not significant ($p > 0.05$).

(**i-k**) Identification of key residues in MRGPRX4 that mediate ligand binding and receptor activation. (**i**) Primary sequence alignment of the human MRGPRX1, MRGPRX2, MRGPRX3, and MRGPRX4 proteins. The positions of the three amino acids in MRGPRX4 that were mutated to alanine are shown at the right. (**j**) Dose-dependent activation of wild-type (WT) MRGPRX4 and three MRGPRX4 mutants with the indicated point mutations was measured using the TGFα shedding assay. n = 1 experiment performed in triplicate. (**k**) Plasma membrane expression of Myc-tagged WT and mutant MRGPRX4 was measured using an anti-Myc antibody and normalized to WT MRGPRX4 expression.

Fig. 4. A subset of human DRG neurons express MRGPRX4 and respond to bile acids.

(**a-d**) Representative DRG sections showing *in situ* hybridization (ISH, **a**) and immunohistochemistry (IHC, **b**) for MRGPRX4; the summary data are shown in (**c**); n = 2234 and 2735 neurons for ISH and IHC, respectively. The scale bars represent 200 μm (**a**) and 100 μm (**b**). (**d**) Diameter distribution for all 2234 DRG neurons

measured using *in situ* hybridization, 124 MRGPRX4-positive neurons, and 788 TrkA-positive neurons.

(**e**) Flow chart depicting the steps for characterizing the gene expression profiles of human DRG samples using triple-color RNAscope *in situ* hybridization.

(**f**) Representative RNAscope images of *MRGPRX4* and other genes in human DRG sections. Each fluorescent dot indicates a single mRNA transcript. Scale bar, 10 μm.

(**g**) Quantification of the gene expression data shown in (**f**). A neuron was defined as positive if $\geq$ 20 fluorescent dots in the respective mRNA channel were detected in that neuron.

(**h**) Bile acids induced a Ca^{2+} response in a subset of cultured human DRG neurons. (**left**) Representative bright-field images and Fluo-8 fluorescence images of two different DRG cultures from one embryo donor one adult donor. (**right**) Representative traces of individual DCA-responsive DRG neurons (circled by the dash line in (**left**)). Pseudo-color images of chemical-induced signals are shown under each trace. C15 (compound 15), CA, DCA, and His (histamine): 100 μM each; KCl: 75 mM. Veh, vehicle. Scale bar, 50 μm.

(**i**) Percentage of human DRG neurons that were responsive to the indicated tested compounds measured as in (**h**).

(**j**) Venn diagram of the cultured human DRG neurons that were activated by the indicated tested compounds. Green represents DCA responded neurons; Heavy gray represents capsaicin responded neurons; light gray represents histamine responded neurons.

Fig. 5 Bile acids and MRGPRX4 specific agonist induce histamine-independent itch in human.

(a1-a2) Itch evoked by a double-blind intradermal injection of DCA and nateglinide (Nat) in human subjects. (25 μl for each injection) (**a1**) Time course of the perceived itch intensity (n = 18-32). The traces are plotted with the standard error of the mean (s.e.m.) at the peak of each trace. The descriptions of the itch intensity are shown on the right. The injection sites on the subject's forearm are indicated. X4, MRGPRX4 (**a2**) Summary of the area-under-the-curve (AUC) of the itch intensity traces shown in (**a1**).

(b1-b2) Itch evoked by the indicated doses of DCA (25 μl for each injection, n = 8-14). The linear regression analysis of concentration versus the AUC is showed as a red line.

(c1-c2) Itch evoked by CDCA, CA, TCDCA, and LCA (25 μl for each injection, n = 10-31). The vehicle data (Veh) is reproduced from (**a1**).

(d1-d2) DCA-evoked itch is not inhibited by antihistamine (Anti-His). (**d1**) Time course of itch intensity evoked by an intradermal injection of DCA or histamine (His) following antihistamine or placebo pretreatment (25 μl for each injection, n = 12-14). Each pair of dots connected by a gray line represents an individual subject.

Student's *t*-test, $^{**}p < 0.01$, $^{***}p < 0.001$, and n.s. = not significant ($p > 0.05$).

Fig. 6 TGR5 does not serve as an itch receptor in human

(**a1-a2**) Intradermal injection of a non-bile acid TGR5 agonist compound 15 (C15) does not induce itch in human. (**a1**) Time course of the perceived intensity of itch evoked by DCA and vehicle are reproduced from **Fig. 5a1**, and the itch evoked by C15 is from 19 subjects. The equivalent concentration (equiv. conc.) of DCA and C15 means the fold of concentration to the EC_{50} of activating human TGR5. (**a2**) The quantification results of area under curve (AUC) of itch intensity shown in (**a1**) (mean ± s.e.m.). Veh, vehicle. Student's t-test, ***p < 0.001, and n.s. not significant (p > 0.05).

(**b-c**) The activation of human MRGPRX4 (**b**) or human TGR5 (**c**) by DCA (red), compound 15 (C15, green) and nateglinide in MRGPRX4- or TGR5-expressing HEK293T cells detected by FLIPR and luciferase assay respectively..

(**d**) The relationship between the evoked itch and the relative potency to activate human MRGPRX4 or human TGR5 by the specific agonists of these two receptors. The Y-axis shows the relative activation of certain compound to the receptor, representing the logarithm of (maximal response/EC_{50}). The X-axis shows the human itch intensity, representing the AUC of itch evoked by certain compound. Statistic test was performed between the itch intensity of compound 15 and vehicle, or between the itch intensity of nateglinide and vehicle. Nat, nateglinide; C15, compound 15; Veh, vehicle. Student's *t*-test, **p < 0.01, and n.s. not significant (p > 0.05).

(**e**) *In situ* hybridization (ISH) of TGR5 in human DRG sections. (**left**) The diagram depicting the morphology of DRG neurons and surrounding satellite glial cells.

592 (**middle and right**) TGR5 was highly expressed in satellite glial cells (indicated by
593 arrows) but not DRG neurons in human DRG. Scale bar, 50 μm
594 (**f**) *In situ* hybridization of TGR5 in mouse DRG sections. TGR5 was highly expressed
595 in DRG neurons (indicated by arrow heads) in mouse DRG. Scale bar, 50 μm
596 (**g-h**) Immunohistochemistry (IHC) of human and mouse DRG sections. (**g**) In human
597 DRG, TGR5 was expressed in satellite glial cells (indicated by arrows) but not in
598 neurons (marked by NeuN, indicated by arrow heads). (**h**) In mouse DRG, TGR5 was
599 expressed in neurons (marked by NeuN, indicated by arrow heads). Scale bar, 50 μ
600 m.
601 (**i**) Quantification of the percentage of TGR5+ neurons (over NeuN+ neurons) in
602 human and mouse DRG (immunohistochemistry). Chi-square test, $^{**}p < 0.01$.
603
604 **Fig. 7 Elevated bile acids are correlated with the occurrence of itch among**
605 **patients with liver disease and are sufficient to activate MRGPRX4.**
606 (**a-b**) Summary of individual bile acid levels (**a**) and total bile acid levels (**b**, the sum of
607 the 12 bile acids shown in **a**) in itchy patients with liver diseases (Liver_itch, n = 27),
608 non-itchy patients liver diseases, (Liver_non-itch, n = 36), and itchy patients with
609 dermatic diseases (Skin_itch, n = 8). The plasma bile acid levels were measured
610 using HPLC-MS/MS (inset).
611 (**c-d**) Summary of individual bile acid levels (**c**) and total bile acid levels (**d**, the sum of
612 the 12 bile acids shown in **c**) in 13 patients with liver diseases during itch and after
613 itch relief. The inset shows the separation of standard bile acids by HPLC-MS/MS.

(**e-f**) Left, Ca^{2+} responses in MRGPRX4-expressing HEK293T cells induced by application of a mixture of artificial bile acids derived from itchy patients with liver diseases and healthy subjects. The Ca^{2+} signal was measured using Fluo-8 and was normalized to the signal measured using the 1x liver_itch mix. The summary data are shown in (**f**); n = 50 cells each.

(**g**) Proposed model depicting the mechanism underlying itch in patients with liver diseases. In itchy patients, accumulated bile acids reach the skin via the circulatory system, where they activate nerve fibers in a subset of MRGPRX4-expressing DRG neurons. These activated neurons relay the itch signal to the spinal cord and higher brain centers, eliciting the sensation of itch.

Student's *t*-test, $*p < 0.05$, $**p < 0.01$, $***p < 0.001$.

Supplementary figures

Supplementary Fig. 1 Construct design and surface expression of candidate GPCRs in HEK293T cells.

(**a**) Map of the generic GPCR expression vector. The 3' and 5' terminal repeats (TR) are recognized by the PiggyBac transposase. Myc, Myc tag; $Puro^R$, puromycin-resistance gene.

(**b**) Plasma membrane expression of the indicated GPCRs transiently expressed in HEK293T cells, detected using an anti-Myc antibody. Scale bar, 20 μm.

Supplementary Fig. 2 ^{1}H-NMR analysis of bile acids in fractions F1, F2, F3, F4, and F6

The hydrogen chemical shift of CA, CDCA, DCA, and LCA at carbon 3, 7, 12 were determined by ^{1}H-NMR. Note that the active fractions (F2 through F4) contained the characteristic hydrogen peaks corresponding to these bile acids.

Supplementary Fig. 3 Human MRGPRX4, but not human MRGPRX1-3 or mouse and rat Mrgpr family members, are activated by bile acids.

(**a**) Phylogenetic analysis of mouse (Mm, green), rat (Rn, blue), rhesus monkey (Rh, black), and human (Hs, red) Mas-related GPCR (mrg) family members. Amino acid sequence similarity compared to Hs. MRGPRX4 is shown in the parenthesis.

(**b-f**) Activation of human MRGPRX1-4 by CA, CDCA, DCA, LCA and Nateglinide (100 μM each, n = 100 cells from two experiments). Human MRGPRX1-4 were stably expressed in HEK293T cells, and activation was measured using the Ca^{2+} indicator Fluo-8. Responses are normalized to Bam8-22 (20 μM), PAMP9-20 (20 μM), ATP (50 μ M), and DCA (100 μ M) for MRGPRX1, MRGPRX2, MRGPRX3, and MRGPRX4, respectively. The data for MRGPRX4 (**e**) are reproduced from **Fig. 3f**.

(**g-h**) Mouse and rat Mrgpr family members are not activated by DCA (100 μM, n = 6 cells) or a mixture of DCA and LCA mix (20 μM each, n = 50 cells).

Supplementary Fig. 4 The anti-MRGPRX4 antibody has high specificity.

HEK293T cells were transiently transfected with MRGPRX1, MRGPRX2, MRGPRX3, or MRGPRX4. The anti-MRGPRX4 antibody (Abcam, ab120808, 1:200 dilution) specifically labeled MRGPRX4-expressing HEK293T cells, but not MRGPRX1-, MRGPRX2-, or MRGPRX3-expressing cells. Transfected cells were identified by mCherry fluorescence, and the nuclei were counterstained with DAPI. Scale bar, 50 μm.

Supplementary Fig. 5 Expressing MRGPRX4 in cultured rat DRG neurons renders the cells responsive to bile acids.

(**a**) Top, cultured rat DRG neurons were transfected with the pPiggyBac-CAG-MRGPRX4-P2A-mCherry plasmid by electroporation. The cells circled by dashed lines are an MRGPRX4-positive neuron (neuron 2 with red fluorescence) and an MRGPRX4-negative (neuron 1) neuron. Bottom, non-transfected cultured rat DRG neurons. A representative neuron (neuron 3) is circled by a dash line. Scale bar, 50 μm.

(**b**) Representative traces from the cells indicated in (**a**). DCA and CA: 10 μM; capsaicin (Cap): 1 μM; KCl: 75 mM.

(**c**) Summary of the amplitude and percentage of Ca^{2+} signals in response to DCA and CA. Responsive neurons were defined as exceeding a threshold of 20% $\Delta F/F_0$. n = 60-77 neurons per group.

(**d**) Summary of the amplitude and percentage of Ca^{2+} signals in response to capsaicin and KCl. Responsive neurons were defined as in (**c**). n = 67-95 neurons per group.

Student's *t*-test or two-proportion z-test, **p* < 0.05, ***p* < 0.01, ****p* < 0.001, and n.s. = not significant (*p* > 0.05).

Supplementary Fig. 6 Cultured human DRG neurons respond to various chemicals.

Ca^{2+} imaging of human DRG neurons from one human embryo (donor 1) and three adult donors (donors 2-4).

(**a**) Representative bright-field and fluorescence images of cultured human DRG neurons. Scale bar, 50 μm.

(**b**) Representative Ca^{2+} traces in response to the indicated test compounds measured in the cells shown in (**a**). Veh, vehicle. Compound 15 (C15), CA and DCA: 100 μM; histamine (His): 50 μM; capsaicin (Cap): 1 μM; KCl: 75 mM.

(**c**) Summary of the percentage of neurons that responded to the indicated test compounds (defined as exceeding a threshold of > 20% $\Delta F/F_0$).

Supplementary Fig. 7 Expression of TGR5 in mouse and monkey DRG

(**a**) Phylogenetic analysis of mouse (Mm.), rat (Rn.), rhesus monkey (Rh,) and human (Hs,) TGR5. Amino acid sequence similarity compared to Hs. TGR5 is shown in the parenthesis.

(**b**) The HEK293T cells were transiently transfected with human TGR5 expression vector (pPiggyBac-TGR5-P2A-mCherry). The anti-TGR5 antibody can specifically labeled the TGR5-expressing cells identified by the mCherry signal. The nuclei were counterstained with DAPI. Arrow heads indicate the representative TGR5-expressing cells. Scale bar, 20 μm.

(**c**) *In situ* hybridization (ISH) of TGR5 in mouse showing the morphology of mouse DRG and the adjacent spinal cord. Scale bar, 100 μm.

(**d**) *In situ* hybridization of TGR5 in monkey (*Macaca mulatta*) DRG sections. TGR5 was highly expressed in satellite glial cells (indicated by arrows). Scale bar, 50 μm

(**e**) Immunohistochemistry (IHC) of monkey DRG sections. TGR5 was expressed in satellite glial cells (indicated by arrows) but not neurons (marked by NeuN, indicated by arrow heads). Scale bar, 50 μm.

Supplementary Fig. 8 Quantification of bile acids in human plasma

(**a**) Standard curve of 12 bile acids quantified by HPLC-MS/MS. All the 12 bile acids show good linear correlation between the MS response and the concentration (0.1-1 μM)

(**b**) Quantification results of 8 bile acids shown in **Fig. 7a**.

(**c**) Quantification results of 8 bile acids shown in **Fig. 7c**.

All error bars represent the s.e.m.; student's *t*-test, $*p < 0.05$, and n.s. = not significant ($p > 0.05$).

Supplementary Fig 9. Bilirubin potentiates the activation of MRGPRX4 by bile acids and may contribute to cholestatic itch.

(**a**) Comparison of the activation of MRGPRX4 by DCA, bilirubin and taurine conjugated bilirubin. Taurine conjugated bilirubin was used in order to mimic the direct bilirubin under human physiological condition. MRGPRX4 was expressed in HEK293T cells and the activation was measured by FLIPR assay.

(**b**) Bilirubin allosterically modulates the activation of MRGPRX4 by DCA. Different concentrations of bilirubin was mixed with DCA, and then the activation of MRGPRX4 by these mixes was tested in MRGPRX4-expressing HEK293T cells using FLIPR assay.

(**c**) DCA allosterically modulates the activation of MRGPRX4 by bilirubin, similar to (**b**).

(**d**) Comparison of total bilirubin, direct bilirubin (conjugated) and indirect bilirubin (unconjugated) level in liver disease patients with itch (Liver_itch) (n = 30) or without itch (Liver_Non-itch) (n = 34), or patients with dermatic itch (Skin_itch) (n = 6).

(**e**) Comparison of total bilirubin, direct bilirubin and indirect bilirubin level in liver disease patients (n=12) during itch and after itch relief.

(**f**) Correlation between itch intensity and plasma total bile acid, total bilirubin, direct bilirubin, and indirect bilirubin. The itch intensity was directly reported by patients via a questionnaire with 0 representing no itch and 10 the highest level of itch.

All error bars represent the s.e.m.. (**a-c**) One-way ANOVA, *p < 0.05, **p < 0.01, ***p < 0.001, and n.s. not significant (p > 0.05). (**d-f**) Student's t-test, **p < 0.01, ***p < 0.001, and n.s. = not significant (p > 0.05).

Supplementary Table. 1 Genes that are highly expressed in human DRG

Supplementary Table 2 GPCRs expression profiling in human DRG

Red labeled genes are candidate GPCRs that are highly expressed in human DRG. Blue labeled gene is TGR5.

References

1 Koch, S. C., Acton, D. & Goulding, M. Spinal Circuits for Touch, Pain, and Itch. *Annu Rev Physiol* **80**, 189-217, doi:10.1146/annurev-physiol-022516-034303 (2018).

2 Tajiri, K. & Shimizu, Y. Recent advances in the management of pruritus in chronic liver diseases. *World J Gastroenterol* **23**, 3418-3426, doi:10.3748/wjg.v23.i19.3418 (2017).

3 Thurmond, R. L., Gelfand, E. W. & Dunford, P. J. The role of histamine H1 and H4 receptors in

allergic inflammation: the search for new antihistamines. *Nat Rev Drug Discov* **7**, 41-53, doi:10.1038/nrd2465 (2008).

4 Beuers, U., Kremer, A. E., Bolier, R. & Elferink, R. P. Pruritus in cholestasis: facts and fiction. *Hepatology* **60**, 399-407, doi:10.1002/hep.26909 (2014).

5 Imam, M. H., Gossard, A. A., Sinakos, E. & Lindor, K. D. Pathogenesis and management of pruritus in cholestatic liver disease. *J Gastroenterol Hepatol* **27**, 1150-1158, doi:10.1111/j.1440-1746.2012.07109.x (2012).

6 Jenkins, J. K. & Boothby, L. A. Treatment of itching associated with intrahepatic cholestasis of pregnancy. *Ann Pharmacother* **36**, 1462-1465, doi:10.1345/aph.1A479 (2002).

7 Kremer, A. E., Oude Elferink, R. P. J. & Beuers, U. Pathophysiology and current management of pruritus in liver disease. *Clinics and Research in Hepatology and Gastroenterology* **35**, 89-97, doi:10.1016/j.clinre.2010.10.007 (2011).

8 Alemi, F. *et al.* The TGR5 receptor mediates bile acid-induced itch and analgesia. *J Clin Invest* **123**, 1513-1530, doi:10.1172/JCI64551 (2013).

9 Lieu, T. *et al.* The bile acid receptor TGR5 activates the TRPA1 channel to induce itch in mice. *Gastroenterology* **147**, 1417-1428, doi:10.1053/j.gastro.2014.08.042 (2014).

10 Cipriani, S. *et al.* Impaired Itching Perception in Murine Models of Cholestasis Is Supported by Dysregulation of GPBAR1 Signaling. *PLoS One* **10**, e0129866, doi:10.1371/journal.pone.0129866 (2015).

11 Meixiong, J. *et al.* Identification of a bilirubin receptor that may mediate a component of cholestatic itch. *Elife* **8**, doi:10.7554/eLife.44116 (2019).

12 Belmonte, C. & Viana, F. Molecular and cellular limits to somatosensory specificity. *Mol Pain* **4**,

14, doi:10.1186/1744-8069-4-14 (2008).

13 Dong, X. & Dong, X. Peripheral and Central Mechanisms of Itch. *Neuron* **98**, 482-494, doi:10.1016/j.neuron.2018.03.023 (2018).

14 Flegel, C., Manteniotis, S., Osthold, S., Hatt, H. & Gisselmann, G. Expression profile of ectopic olfactory receptors determined by deep sequencing. *PLoS One* **8**, e55368 (2013).

15 Flegel, C. *et al.* RNA-seq analysis of human trigeminal and dorsal root ganglia with a focus on chemoreceptors. *PLoS One* **10**, e0128951 (2015).

16 Liu, Q. *et al.* Sensory neuron-specific GPCR Mrgprs are itch receptors mediating chloroquine-induced pruritus. *Cell* **139**, 1353-1365, doi:10.1016/j.cell.2009.11.034 (2009).

17 Liu, Q. *et al.* Mechanisms of itch evoked by beta-alanine. *J Neurosci* **32**, 14532-14537, doi:10.1523/JNEUROSCI.3509-12.2012 (2012).

18 Hall, M. P. *et al.* Engineered luciferase reporter from a deep sea shrimp utilizing a novel imidazopyrazinone substrate. *ACS Chem Biol* **7**, 1848-1857, doi:10.1021/cb3002478 (2012).

19 Inoue, A. *et al.* TGFalpha shedding assay: an accurate and versatile method for detecting GPCR activation. *Nat Methods* **9**, 1021-1029, doi:10.1038/nmeth.2172 (2012).

20 Patapoutian, A. & Reichardt, L. F. Trk receptors: mediators of neurotrophin action. *Curr Opin Neurobiol* **11**, 272-280 (2001).

21 Han, S. K., Mancino, V. & Simon, M. I. Phospholipase Cbeta 3 mediates the scratching response activated by the histamine H1 receptor on C-fiber nociceptive neurons. *Neuron* **52**, 691-703, doi:10.1016/j.neuron.2006.09.036 (2006).

22 Imamachi, N. *et al.* TRPV1-expressing primary afferents generate behavioral responses to pruritogens via multiple mechanisms. *PNAS* **106**, 11330 –11335 (2009).

807 23 Wilson, S. R. *et al.* TRPA1 is required for histamine-independent, Mas-related G
808 protein-coupled receptor-mediated itch. *Nat Neurosci* **14**, 595-602, doi:10.1038/nn.2789
809 (2011).
810 24 Usoskin, D. *et al.* Unbiased classification of sensory neuron types by large-scale single-cell
811 RNA sequencing. *Nat Neurosci* **18**, 145-153, doi:10.1038/nn.3881 (2015).
812 25 Li, C. L. *et al.* Somatosensory neuron types identified by high-coverage single-cell
813 RNA-sequencing and functional heterogeneity. *Cell Res* **26**, 83-102, doi:10.1038/cr.2015.149
814 (2016).
815 26 Green, B. G. *et al.* Evaluating the 'Labeled Magnitude Scale' for Measuring Sensations of
816 Taste and Smell. *Chemical Senses* **21**, 323–334 (1996).
817 27 Kroeze, W. K. *et al.* PRESTO-Tango as an open-source resource for interrogation of the
818 druggable human GPCRome. *Nat Struct Mol Biol* **22**, 362-369, doi:10.1038/nsmb.3014 (2015).
819 28 J. KIRBY, K. W. H., J. L. BURTON. Pruritic Effect of Bile Salts. *British Medical Journal* **4**,
820 693-695 (1974).
821 29 Varadi, D. P. Pruritus Induced by Crude Bile and Purified Bile Acids. *Arch Dermatol* **109**
822 (1974).
823 30 Hogenauer, K. *et al.* G-protein-coupled bile acid receptor 1 (GPBAR1, TGR5) agonists reduce
824 the production of proinflammatory cytokines and stabilize the alternative macrophage
825 phenotype. *J Med Chem* **57**, 10343-10354, doi:10.1021/jm501052c (2014).
826 31 Neale, G., Lewis, B., Weaver, V. & Panveliwalla, D. Serum bile acids in liver disease. *Gut* **12**,
827 145-152 (1971).
828 32 Freedman, M. R., Holzbach, R. T. & Ferguson, D. R. Pruritus in cholestasis no direct causative

role for bile acid retention. *The American Journal of Medicine* **70**, 1011-1016 (1981).

33 Bartholomew, T. C., Summerfield, J. A., Billing, B. H., Lawson, A. M. & Setchell, K. D. Bile acid profiles of human serum and skin interstitial fluid and their relationship to pruritus studied by gas chromatography-mass spectrometry. *Clin Sci (Lond)* **63**, 65-73 (1982).

34 Leslie Schoenfield & Sjovall, J. Bile acids on the skin of patients with pruritus hepatobiliary disease. *Nature* **January 7**, 93-94 (1967).

35 Xiang, X. *et al.* High performance liquid chromatography-tandem mass spectrometry for the determination of bile acid concentrations in human plasma. *J Chromatogr B Analyt Technol Biomed Life Sci* **878**, 51-60, doi:10.1016/j.jchromb.2009.11.019 (2010).

36 Jenkins, H. H., Spencer, E. D., Weissgerber, A. J., Osborne, L. A. & Pellegrini, J. E. Correlating an 11-point verbal numeric rating scale to a 4-point verbal rating scale in the measurement of pruritus. *J Perianesth Nurs* **24**, 152-155, doi:10.1016/j.jopan.2009.01.010 (2009).

37 Lek, M. *et al.* Analysis of protein-coding genetic variation in 60,706 humans. *Nature* **536**, 285-291, doi:10.1038/nature19057 (2016).

38 Hill, R. NK1 (substance P) receptor antagonists--why are they not analgesic in humans? *Trends Pharmacol Sci* **21**, 244-246 (2000).

39 Mogil, J. S. Animal models of pain: progress and challenges. *Nat Rev Neurosci* **10**, 283-294, doi:10.1038/nrn2606 (2009).

40 Hug, A. & Weidner, N. From bench to beside to cure spinal cord injury: lost in translation? *Int Rev Neurobiol* **106**, 173-196, doi:10.1016/B978-0-12-407178-0.00008-9 (2012).

41 Taneja, A., Di Iorio, V. L., Danhof, M. & Della Pasqua, O. Translation of drug effects from

experimental models of neuropathic pain and analgesia to humans. *Drug Discov Today* **17**, 837-849, doi:10.1016/j.drudis.2012.02.010 (2012).

42 Geenes, V. & Williamson, C. Intrahepatic cholestasis of pregnancy. *World J Gastroenterol* **15**, 2049-2066 (2009).

43 Yusa, K., Zhou, L., Li, M. A., Bradley, A. & Craig, N. L. A hyperactive piggyBac transposase for mammalian applications. *Proc Natl Acad Sci U S A* **108**, 1531-1536, doi:10.1073/pnas.1008322108 (2011).

859 **MATERIALS AND METHODS**

860 ***Analysis of GPCRs expressed in human DRG neurons***

861 The expression profile of all genes in hDRG neurons was compared to human
862 reference tissues, including trigeminal ganglia, brain, colon, liver, lung, muscle, and
863 testis[14,15]. To identify DRG-enriched GPCRs, we using the following formula: [(the
864 expression level of a given gene in the DRG)/(the total expression level of that gene
865 in all tissues)]; a value ≥0.5 was used to define DRG-enriched genes. The expression
866 level of a gene refers to the number of fragments per kilobase of exon per million
867 fragments mapped (FPKM) in the tissue transcriptome.

868

869 ***Bovine tissue extracts***

870 Fresh bovine heart, brain, kidney, spleen, and liver tissues (40 g each) were
871 dissected and then boiled for 5 min in 200 ml water. Acetic acid and HCl were then
872 added to a final concentration of 1 M and 20 mM, respectively, and the mixture was
873 homogenized thoroughly and then centrifuged at 11,000 rpm for 30 min. The
874 supernatant was collected and concentrated to a volume of 40 ml using a rotary
875 evaporator. Acetone (80 ml) was then added to the concentrated solution, and the
876 new solution was again centrifuged at 11,000 rpm for 30 minutes. The supernatant
877 was collected using a rotary evaporator and freeze-dried in a vacuum. The final
878 product was weighed, and equal amounts of each extract were used to test for
879 activity.

880

881 ***Generation of stable GPCR-expressing cell lines***

882 Stable cell lines expressing orphan GPCRs were generated using the PiggyBac
883 Transposon System. In brief, each orphan GPCR was subcloned into the PiggyBac
884 Transposon vector and co-transfected with the hyperactive PiggyBac transposase[43]
885 into the HEK293T-based TGFα shedding reporter cell line[19] using polyethylenimine
886 (PEI). Receptor-expressing cells were selected and maintained in DMEM containing
887 10% fetal bovine serum (FBS), 1 μg/ml puromycin, 100 U penicillin, and 100 μg/ml
888 streptomycin in a humidified atmosphere at 37°C containing 5% CO_2.

889

890 ***TGFα shedding assay***

891 Cultured cells expressing orphan GPCRs were rinsed once with Mg^{2+}-free and
892 Ca^{2+}-free phosphate-buffered saline (PBS) and then detached with 0.05% (w/v)
893 trypsin. The cell suspension was transferred to a 15-ml tube and centrifuged at 190x*g*
894 for 5 min. The supernatant was discarded, and the cell pellet was suspended in 10 ml
895 PBS and incubated for 15 min at room temperature (RT). The cells were
896 re-centrifuged and suspended in 4 ml HBSS (Hanks' balanced salt solution)
897 containing 5 mM HEPES (pH 7.4). The suspended cells were then seeded in a
898 96-well plate at 40,000-50,000 cells per well and placed in a 37ºC incubator in 5%
899 CO_2 for 30 min. A 10x stock solution of each drug was prepared in assay buffer
900 (HBSS containing 5 mM HEPES, pH 7.4), and 10 μl of 10x stock solution was added
901 to each well. The plate was then placed in the incubator for 2 hr, after which alkaline
902 phosphatase (AP) activity was measured in the conditioned media and cells.

903

904 ***FLIPR assay***

905 HEK293T cells stably expressing human MRGPRX4 were seeded in 96-well plates at
906 a density of ~50,000 cells per well. The following day, the cells were loaded with
907 Fluo-8 (Screen Quest Fluo-8 No-Wash Calcium Assay Kit, AAT Bioquest, Cat. No.
908 36316) for 2 hr, and test compounds were added to the wells. The Fluo-8 signal was
909 measured using the FLIPR TETRA system (PerkinElmer).

910

911 ***Luciferase assay***

912 We generated a luciferase reporter plasmid that encodes secreted NanoLuc under
913 the control of a cAMP response element (CRE) and a minimal promoter. The
914 hygromycin-resistance gene and EBFP driven by the SV40 promoter in the reporter
915 plasmid were used to generate stable cell lines. HEK293T cells were transfected with
916 this plasmid, and a stable cell line was generated by selecting with hygromycin.

917 This stable reporter cell line was then transfected with various GPCRs and used
918 to monitor the activation of these receptors. In brief, the cells were seeded in 96-well
919 plates; the next day, the culture medium was replaced, and compounds were added
920 to the wells; forskolin (10 μM final concentration) and 0.01% DMSO (v/v) were used
921 as positive and negative controls, respectively. The plates were incubated at 37°C in
922 5% CO_2 for 24 hr, after which a 10-μl aliquot of cell culture medium was removed from
923 each well and combined with 40 μl culture medium plus 50 μl assay buffer (containing
924 20 μM of the luciferase substrate coelenterazine); after 5 min incubation,

925 luminescence was measured using an EnVision plate reader (PerkinElmer).

926

927 ***Fractionation of bile acid components***

928 A commercially available bovine bile acid powder (126.6 mg) was loaded in a silica
929 gel column (DCM:MeOH = 10:1). The smaller fractions were combined to form six
930 larger fractions (F1 through F6) based on analytical thin-layer chromatography
931 performed using 0.25-mm silica gel 60-F plates. Flash chromatography was
932 performed using 200−400 mesh silica gel.

933

934 ***MS and NMR***

935 High-resolution mass spectrometry was performed at the Peking University Mass
936 Spectrometry Laboratory using a Bruker Fourier Transform Ion Cyclotron Resonance
937 Mass Spectrometer Solarix XR. ^{1}H-NMR spectra were recorded on a Bruker
938 400-MHz spectrometer at ambient temperature with $CDCl_3$ as the solvent.

939

940 **Immunostaining and flow cytometry analysis**

941 Suspended live HEK 293 cells stably expressing the point-mutated MRGPRX4 were
942 washed in washing buffer (1X PBS solution, mixed with 5% fatal bovine serum (FBS))
943 for 3 times. Then cells were incubated with primary antibody (Sigmal-Aldrich Cat. No.
944 C3956, 1:25 dilution) for 30 minutes, and secondary antibody (AAT Bioquest iFluro^{TM}
945 Alexa 488 goat antirabbit IgG Cat. No. 1060423, 1:50 dilution) for 1 hour. Cells were
946 washed for two times after each antibody treatment. Next, cells were resuspended

with 300 uL to 500 uL FACS buffer, and fluorescence-activated cell-sorting analysis was performed, using the BD FACS Calibor Flow cytometer (BD Biosciences), and the data were analyzed using FlowJo software (Ver. 7.6.1).

Cultured human DRG neurons

Collection of DRG tissue from adult humans was approved by the Committee for Medical Science Research Ethics, Peking University Third Hospital (IRB00006761-2015238), and collection from human embryos was approved by the Reproductive Study Ethics Committee of Peking University Third Hospital (2012SZ-013 and 2017SZ-043) and Beijing Anzhen Hospital (2014012x). DRG tissues were obtained from adult patients undergoing surgical excision of a schwannoma; the tissues were placed immediately in ice-cold DMEM/F12 medium. The tissues were then cut into pieces <1 mm in size and treated with an enzyme solution containing 5 mg/ml dispase and 1 mg/ml collagenase at 37°C for 1 hr. After trituration and centrifugation, the cells were washed in 15% (w/v) bovine serum albumin (BSA) resuspended in DMEM/F12 containing 10% FBS, plated on glass coverslips coated with poly-D-lysine and laminin, cultured in an incubator at 37°C, and used within 24 hr of plating.

Culture and electroporation of rodent DRG neurons

Rat DRG tissues were obtained from the thoracic and lumbar vertebrae and placed in ice-cold DMEM/F12 medium. The tissues were cut into pieces <1 mm in size and

then treated with an enzyme solution containing 5 mg/ml dispase and 1 mg/ml collagenase at 37°C for 1 hr. After trituration and centrifugation, the cells were washed in 15% BSA, resuspended in DMEM/F12 containing 10% FBS, plated on glass coverslips coated with poly-D-lysine and laminin, cultured in an incubator at 37°C, and used within 24 hr of plating.

Rat DRG neurons were electroporated as follows. After washing the neurons with 15% BSA, the neurons were resuspended in DMEM/F12 and electroporated using a P3 Primary Cell 4D-Nucleofector X Kit L (cat. no. V4XP-3012, Lonza) in accordance with the manufacturer's instructions. After electroporation, the neurons were cultured for 72 hr before use in order to allow the transgenes to express.

Ca^{2+} imaging

For Ca^{2+} imaging experiments, cells were loaded at 37°C for 1 hr with 10 μg/ml Fluo-8 AM (AAT Bioquest, Inc.) supplemented with 0.01% Pluronic F-127 (w/v; Invitrogen). Bile acids, bio-mimicked bile acid mixes, and/or various drugs to be tested were added to the cells in a chamber containing a custom-made 8-channel perfusion valve control system. Fluorescence images were acquired using a Nikon A1 confocal microscope.

In situ hybridization and immunostaining

Single colorimetric *in situ* hybridization in hDRG sections was performed as follows. The sections were fixed in freshly prepared 4% paraformaldehyde (PFA) in PBS for

20 min at RT, and then washed in fresh-DEPC PBS (1:1000 DEPC was added to 1x PBS immediately before use) and DEPC-pretreated PBS (1:1000 DEPC in PBS overnight, followed by autoclaving) for 10 min each. The sections were then immersed in a DEPC-containing antigen-retrieval solution containing 10 mM citric acid, 0.05% Tween-20 (pH 6.0) in a 95°C water bath for 20 min, and then cooled at RT for 30 min. After washing in DEPC-pretreated PBS for 10 min, the sections were incubated in a Proteinase K solution (25 µg/mL in DEPC-pretreated water) for 20 min and then washed in fresh-DEPC PBS and DEPC-pretreated PBS (10 min each). The sections were incubated in freshly prepared acetylation solution containing 0.1 M TEA and 0.25% acetic anhydride in DEPC-pretreated water for 10 min at RT, followed by a 10-min wash in DEPC-pretreated PBS. The prehybridization step was performed in probe-free hybridization buffer consisting of 50% formamide, 5x SSC, 0.3 mg/ml yeast tRNA, 100 µg/ml heparin, 1x Denhardt's solution, 0.1% Tween-20, 0.1% CHAPS, and 5 mM EDTA in RNase-free water at 62°C for 30 min in a humidified chamber, followed by an overnight hybridization step in hybridization buffer containing 5 ng/µl DIG-labeled riboprobes at 62°C in a humidified chamber (under a Parafilm coverslip). After the hybridization step, the sections were washed in 0.2x SSC at 68°C (once for 15 min and twice for 30 min each), followed by blocking in PBS containing 0.1% Triton X-100 and 20% horse serum for 1 hr at RT. The sections were then stained overnight at 4°C with pre-absorbed AP-conjugated sheep anti-DIG antibody (1:1000, Roche, cat. 11093274910) in PBS containing 0.1% Triton X-100 and 20% horse serum. The sections were washed 3 times for 10 min each in PBS containing

0.1% Triton X-100, followed by overnight incubation in the dark in AP buffer containing 100 mM Tris (pH 9.5), 50 mM $MgCl_2$, 100 mM NaCl, 0.1% Tween-20, 5 mM levamisole, 0.34 mg/ml NBT (Roche cat. no. 11383213001), and 0.17 mg/ml BCIP (Roche, cat. no. 1138221001) to allow the color reaction to develop. The sections were washed 3 times for 10 min each in PBS, and then fixed for 30 min in 4% PFA in PBS. The sections were quickly rinsed 5 times in ddH_2O, dried at 37°C for 1 hr, and dehydrated in xylene (3 times for 2 min each). Finally, the sections were mounted under a glass coverslip using Permount (Fisher).

Immunostaining was performed using a rabbit anti-hMRGPRX4 antibody obtained (Abcam, cat. no. ab120808). The sections were fixed in freshly prepared 4% PFA in PBS for 20 min at RT and then washed in PBS containing 0.1% Triton X-100 3 times for 10 min each, followed by block in PBS containing 0.1% Triton X-100 and 20% horse serum for 1 hour at RT. The sections were then incubated overnight in primary antibody at 4°C, washed with PBS containing 0.1% Triton X-100 3 times for 15 min each, and incubated with secondary antibody for 1 hour at RT. After washing with PBS 3 times for 15 min each, the sections were mounted under glass coverslips and Fluoromount-G (Invitrogen).

RNAscope in situ hybridization

RNAscope *in situ* hybridization was performed in accordance with the manufacturer's instructions (Advanced Cell Diagnostics). In brief, human DRG sections were fixed, dehydrated, and treated with protease. The sections were then hybridized with the

respective target probe for 2 hours at 40°C, followed by four-round signal amplification. The sections were then mounted under coverslips, sealed with nail polish, and stored in the dark at 4°C until imaged.

Human itch test

The human itch test studies were approved by the Committee for Protecting Human and Animal Subjects at the Department of Psychology, Peking University (#2018-05-02). Volunteers were students and faculty members recruited from Peking University. All subjects provided written informed consent and were provided with the experimental protocol. All injections were performed using an INJEX 30 needle-free injection system (INJEX Pharma GmbH, Berlin, Germany). We performed two studies as described below.

In the first study (to measure bile acid□induced itch sensation), each tested compound was dissolved in physiological saline containing 7% Tween-80 (Sigma-Aldrich). The injection sites were cleaned with rubbing alcohol, and 25 μl of each solution was injected intradermally on the volar surface of each arm. The same volume of vehicle (saline containing 7% Tween-80) served as the negative control. Itch was defined as the desire to initiate scratching during the experiment, and the subjects rate the perceived intensity according the generalized labeled magnitude scale (LMS) described by Green et al.[26]

In the second study (to measure the effect of antihistamines on DCA-induced itch), two experimental sessions were performed, separated by 2 weeks, with 14 and

12 subjects participating in the first and second sessions, respectively. Approximately 1.5 g of topical antihistamine cream (doxepin hydrochloride cream, Chongqing Huapont Pharm. Co., China) or a placebo cream (cold cream, Eau Thermale Avène, Paris, France) was applied 2.5 hr before injection of DCA or histamine (Sigma-Aldrich); any unabsorbed cream was removed with alcohol. A 500 μg/25 μl solution of DCA was prepared as described above, and a 2.5 μg/25 μl solution of histamine was dissolved in saline; 25 μl of the DCA or histamine solution was injected into the volar surface of the arm as described above. In the first session, each subject received two intradermal injections of DCA (one at the antihistamine-treated site and one at the placebo-treated site). In the second session, each subject received two intradermal injections of histamine (one at the antihistamine-treated site and one at the placebo-treated site). The subjects then rate the itch sensation as described above.

Quantification of plasma bile acids and bilirubin

These experiments were approved by the Committee for Biomedical Ethics, Peking University First Hospital (2017-R-94). Itch intensity was measured using a self-report numerical rating scale (NRS)[36], and whole blood samples were collected from patients with skin diseases and patients with liver diseases. Plasma was obtained by centrifuging 2 ml of whole blood at 4°C, 11,000 g for 10 min; 100 μl of each plasma sample was then mixed with 400 μl acetonitrile and left to sit at 4°C for 20 min. The mixture was centrifuged, and the supernatant was dried in a rotatory evaporator

(45°C under vacuum), and the dried residue was retrieved and dissolved in 60% methanol for further analysis.

The bile acid level in plasma samples was measured using HPLC-MS/MS (Agilent model LC1260 QQQ 6495). Chromatographic separation was performed in an ACQUITY UPLC HSS T3 column (2.1 mm × 100 mm, 1.8 µm; Waters Corp.). The mobile phase consisted of solution A (water) and solution B (acetonitrile). The total running time was 23 min, and a linear gradient (0.3 ml/min) was applied as follows: 0-2 min: 10% B - 40% B; 2-18 min: 40% B - 50% B; 18-19 min: 50-100% B; 19-20 min: 100% B; 20-21 min: 100-10% B; 21-23 min: 10% B. The injection volume was 5 µl, and the mobile phase flow rate was 3 ml/min. Deoxycholic-2,2,4,4,11,11-d6 acid (Sigma, cat. no. 809675) was used as an internal standard.

Total bilirubin and direct bilirubin values were obtained from the patients' hospital blood chemistry reports.

Statistical analysis

Summary data are presented as the mean ± SEM. Human subjects were randomly assigned to control and experimental groups, and the subjects and investigators were double-blinded with respect to the experiment treatments. Data were analyzed using the Student's *t*-test, two-proportion z-test, Chi-square test or One-way ANOVA and differences with a *P*-value of < 0.05 were considered significant.

Fig. 1 Identification of MRGPRX4 activated by bile extract.

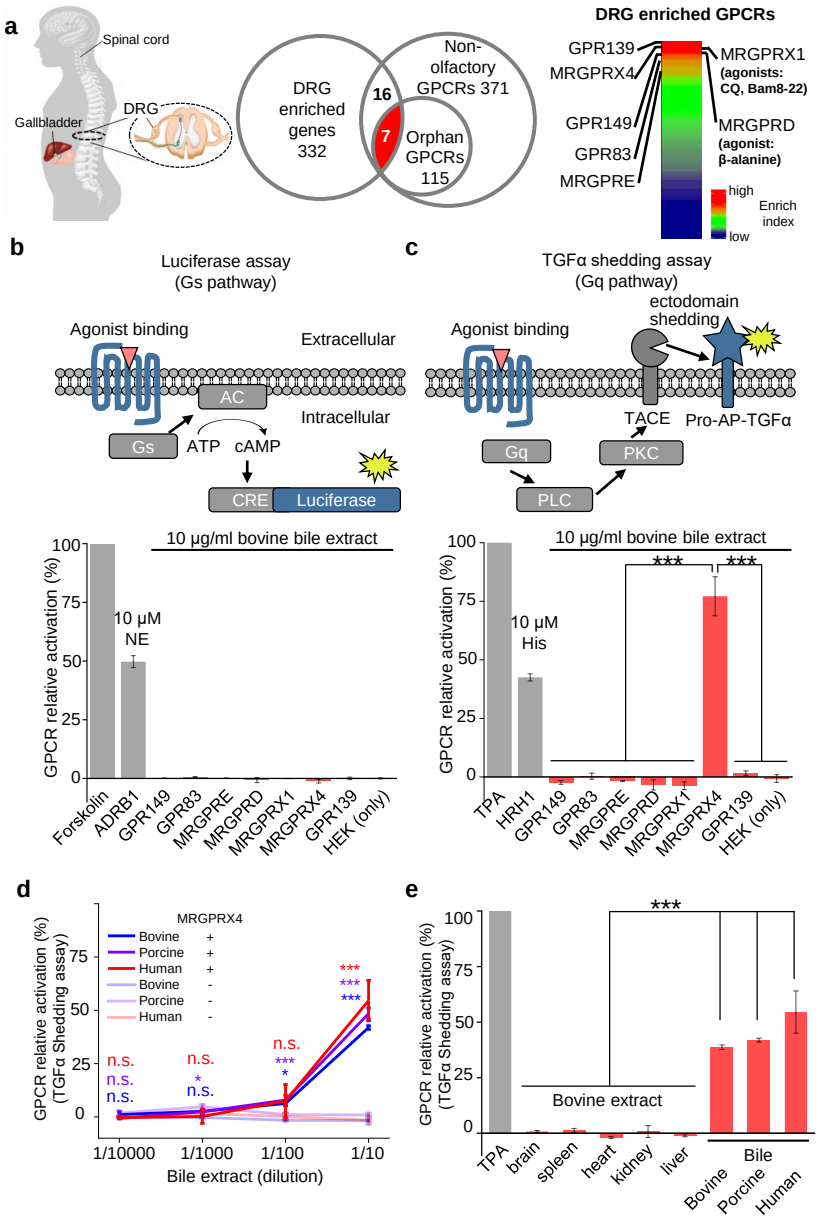

Fig. 2 Identification of active components that activate MRGPRX4 from bile extract.

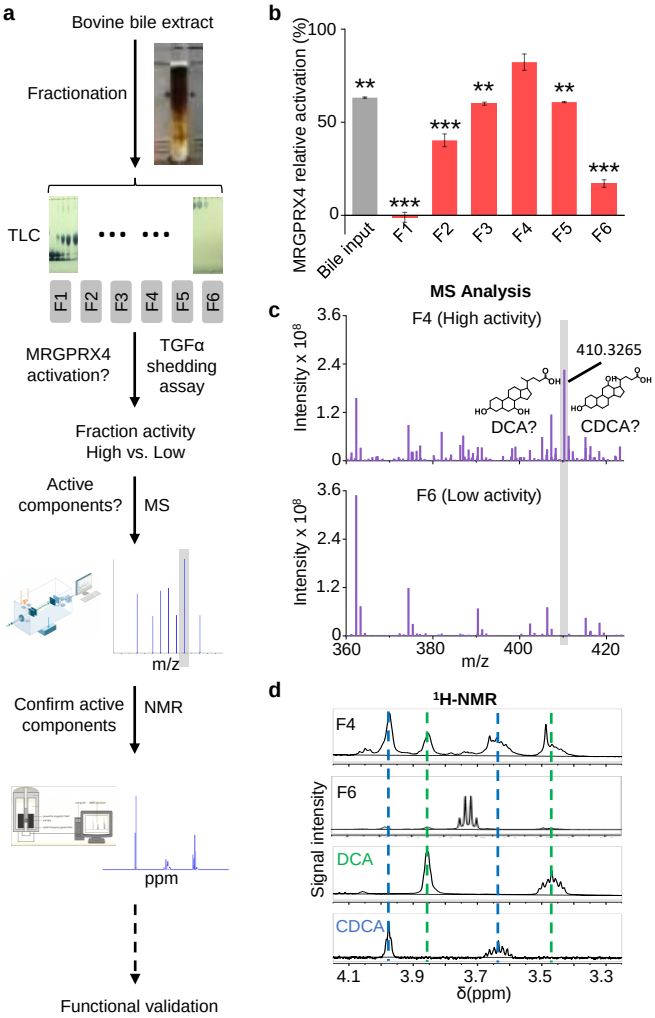

Fig. 3 Functional characterization and molecular profiling of bile acids as ligands for MRGPRX4

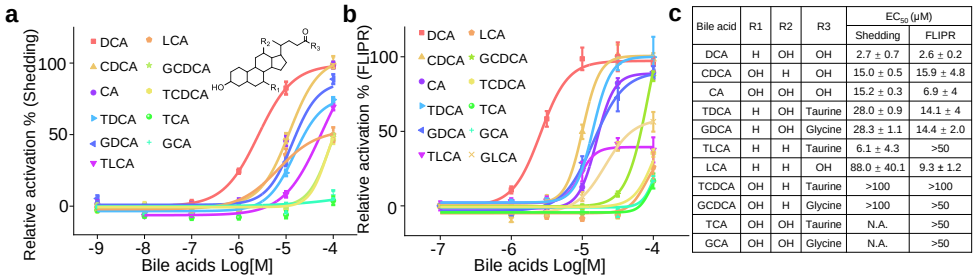

c

Bile acid	R1	R2	R3	EC_{50} (μM)	
				Shedding	FLIPR
DCA	H	OH	OH	2.7 ± 0.7	2.6 ± 0.2
CDCA	OH	H	OH	15.0 ± 0.5	15.9 ± 4.8
CA	OH	OH	OH	15.2 ± 0.3	6.9 ± 4
TDCA	H	OH	Taurine	28.0 ± 0.9	14.1 ± 4
GDCA	H	OH	Glycine	28.3 ± 1.1	14.4 ± 2.0
TLCA	H	H	Taurine	6.1 ± 4.3	>50
LCA	H	H	OH	88.0 ± 40.1	9.3 ± 1.2
TCDCA	OH	H	Taurine	>100	>100
GCDCA	OH	H	Glycine	>100	>50
TCA	OH	OH	Taurine	N.A.	>50
GCA	OH	OH	Glycine	N.A.	>50

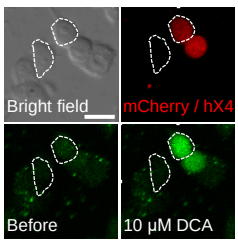

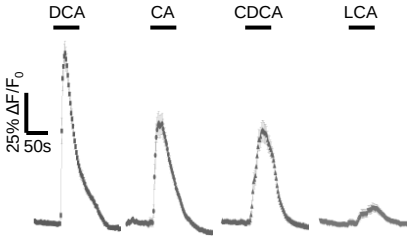

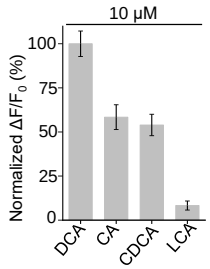

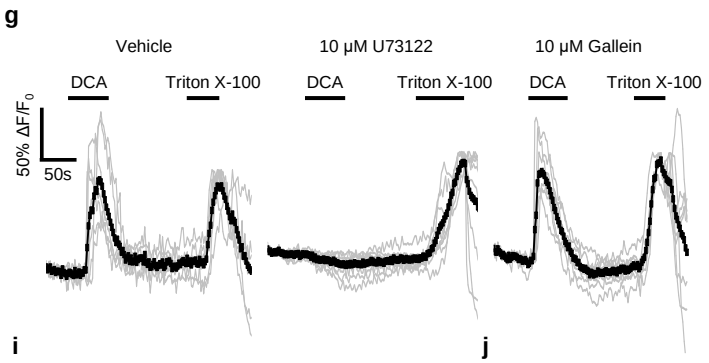

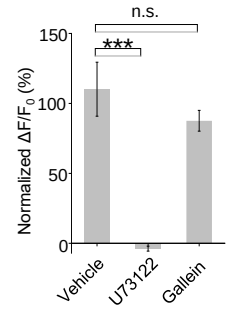

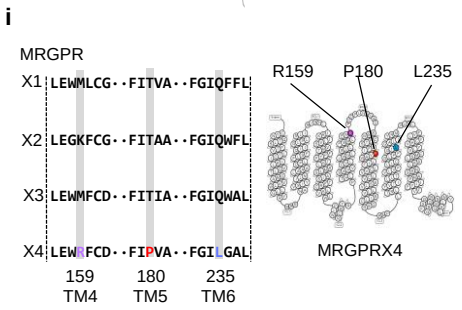

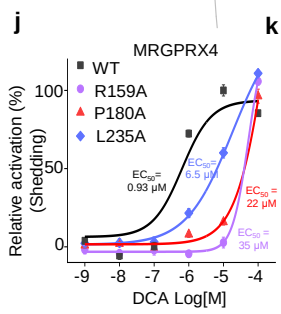

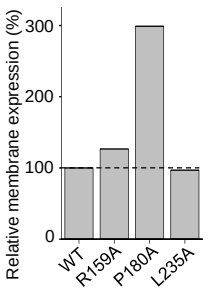

Fig. 4 A subset of hDRG neurons express MRGPRX4 and respond to bile acids.

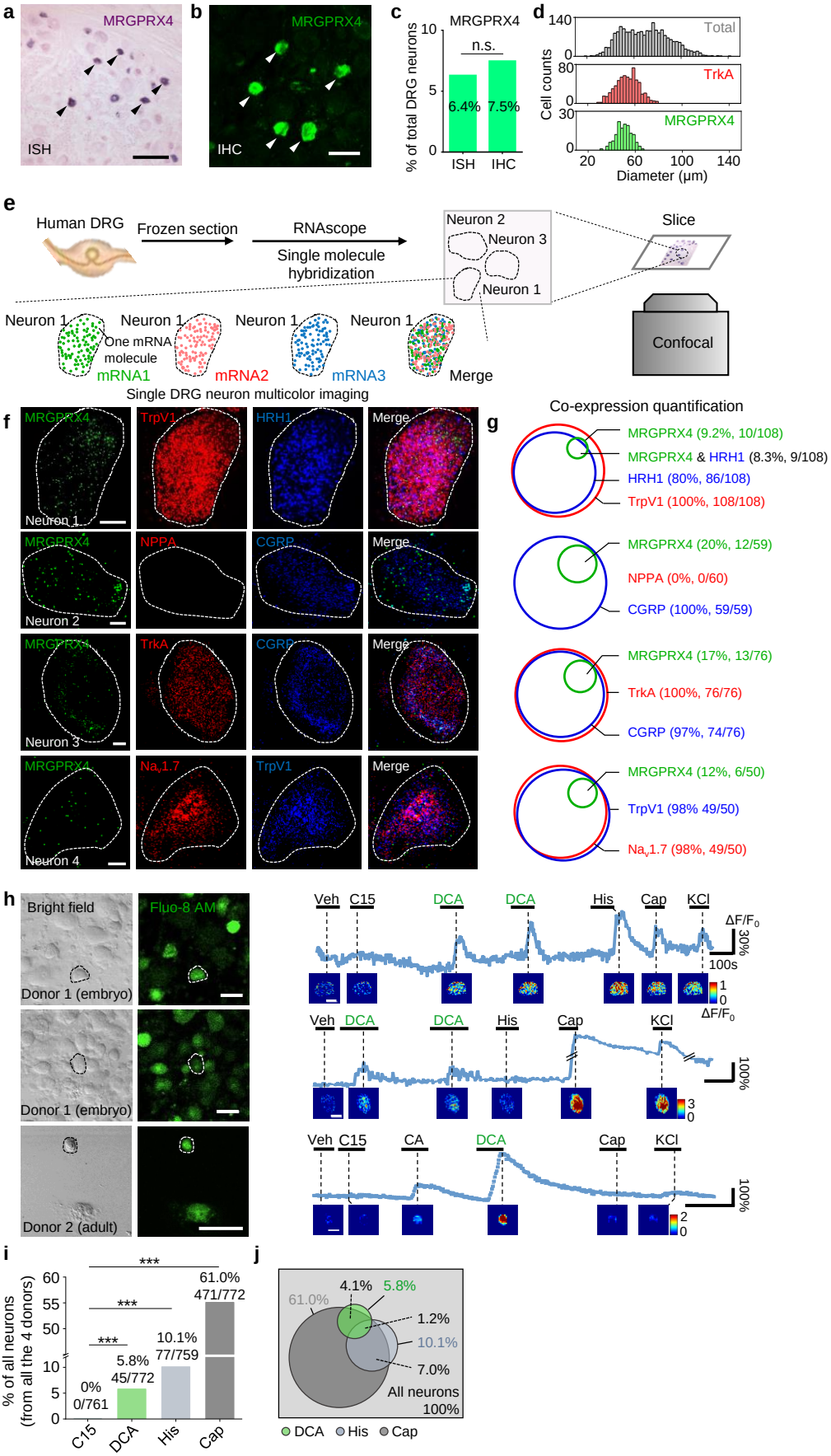

Fig. 5 Bile acids and MRGPRX4 specific agonist induce histamine-independent itch in human

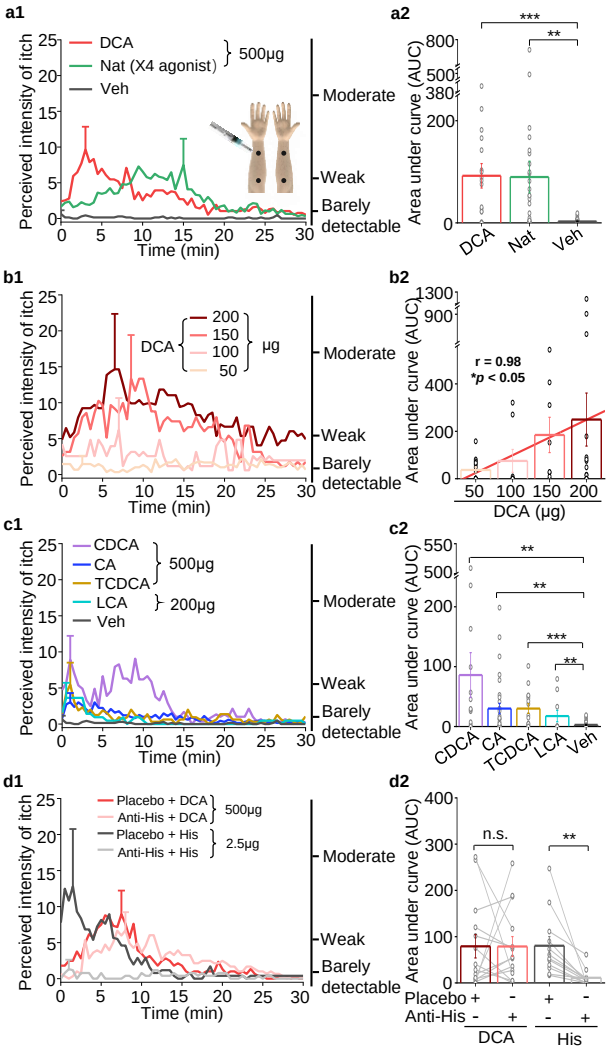

Fig. 6 TGR5 does not serve as an itch receptor in human

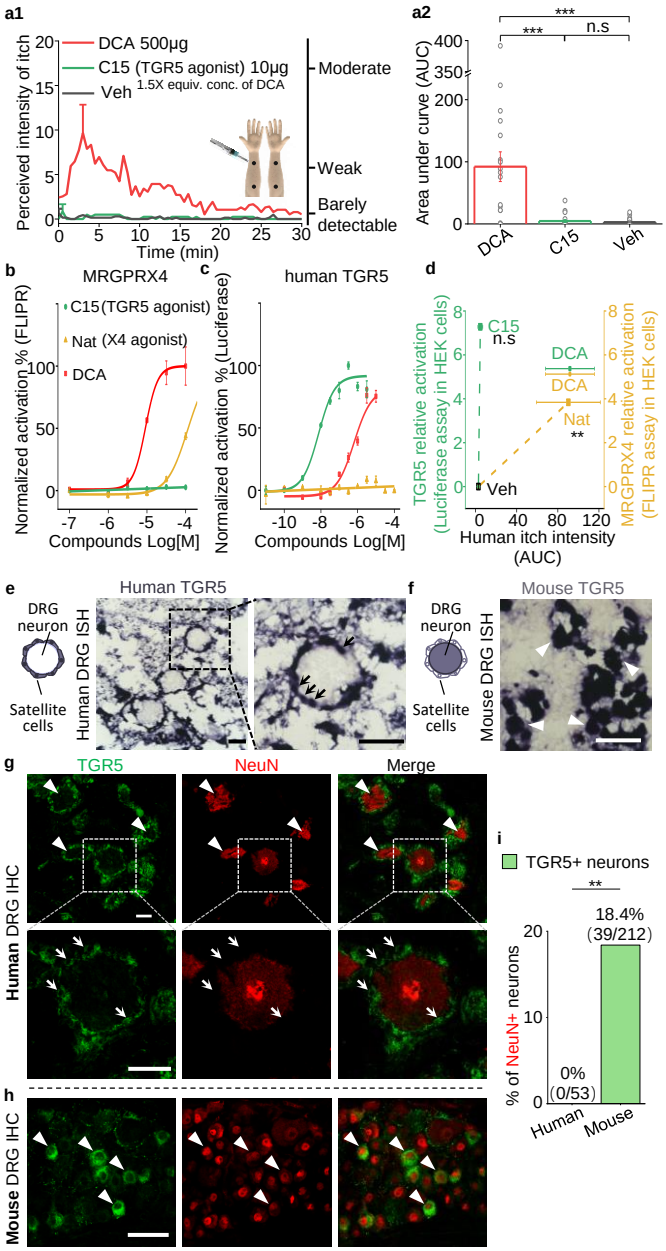

Fig. 7 Elevated bile acids correlate with the occurrence of itch among liver disease patients and are sufficient to activate MRGPRX4

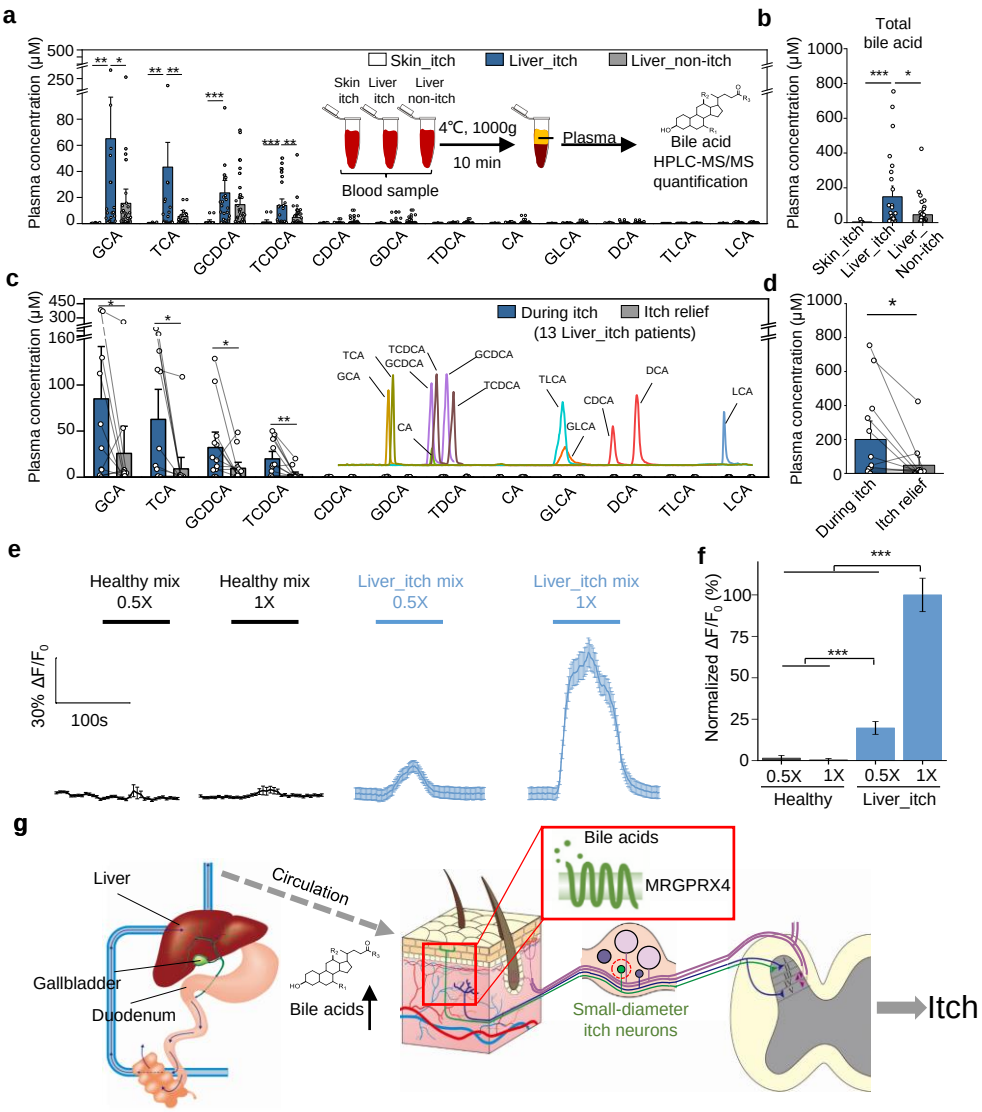

Supplementary Fig. 1 Construct design and surface expression of candidate GPCRs in HEK293T cells

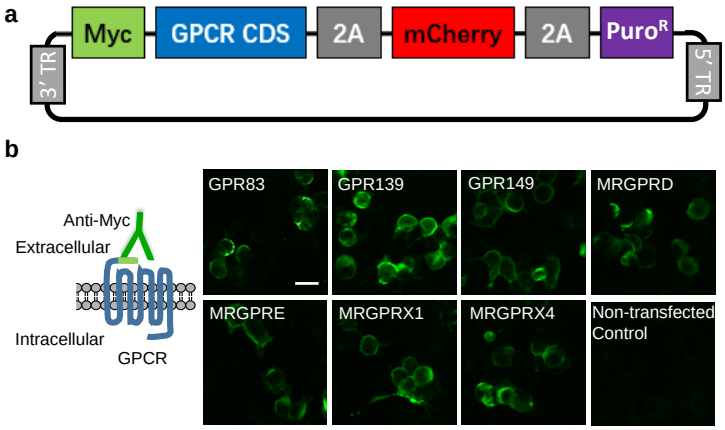

Supplementary Fig. 2 ^{1}H-NMR analysis of bile acids in fractions F1, F2, F3, F4, and F6

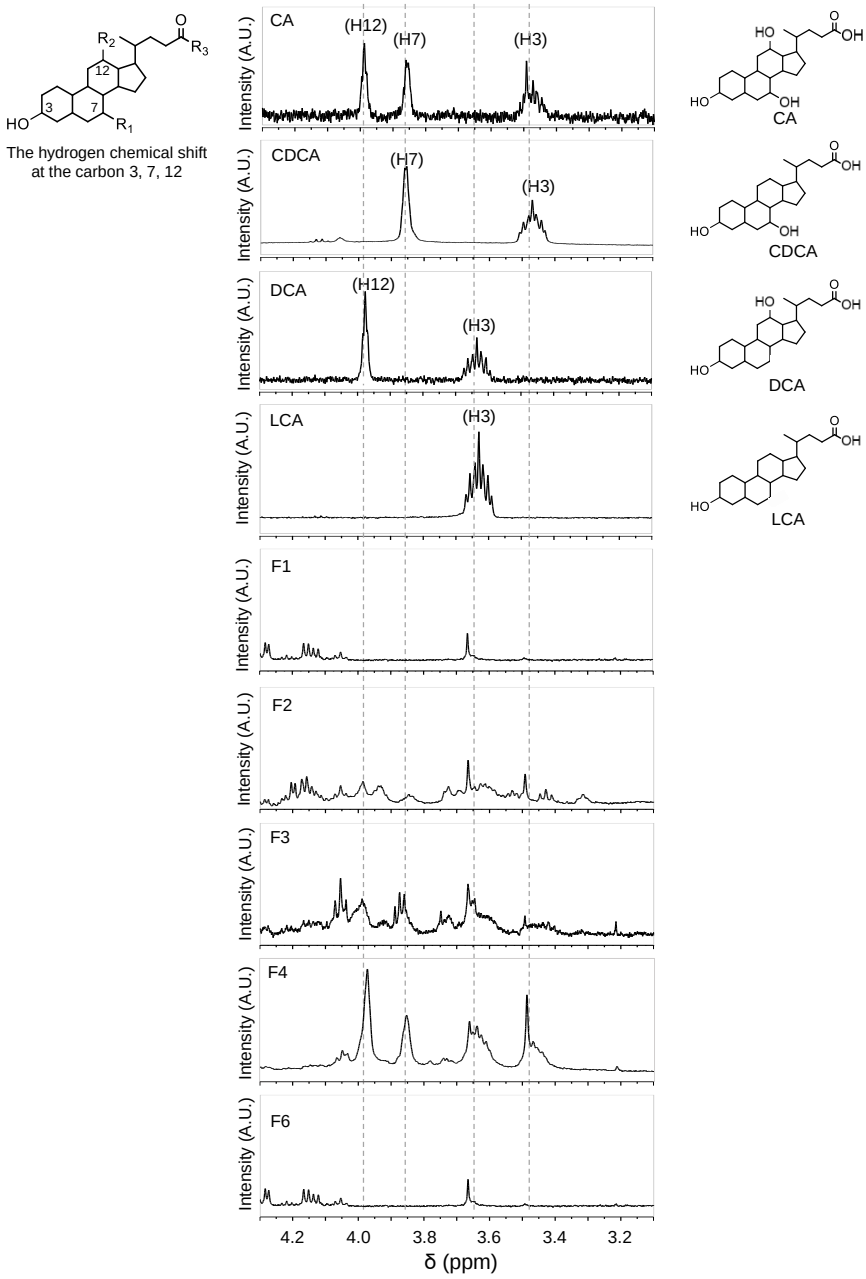

Supplementary Fig. 3 Human MRGPRX4, but not human MRGPRX1-3 or mouse and rat Mrgpr family members, are activated by bile acids.

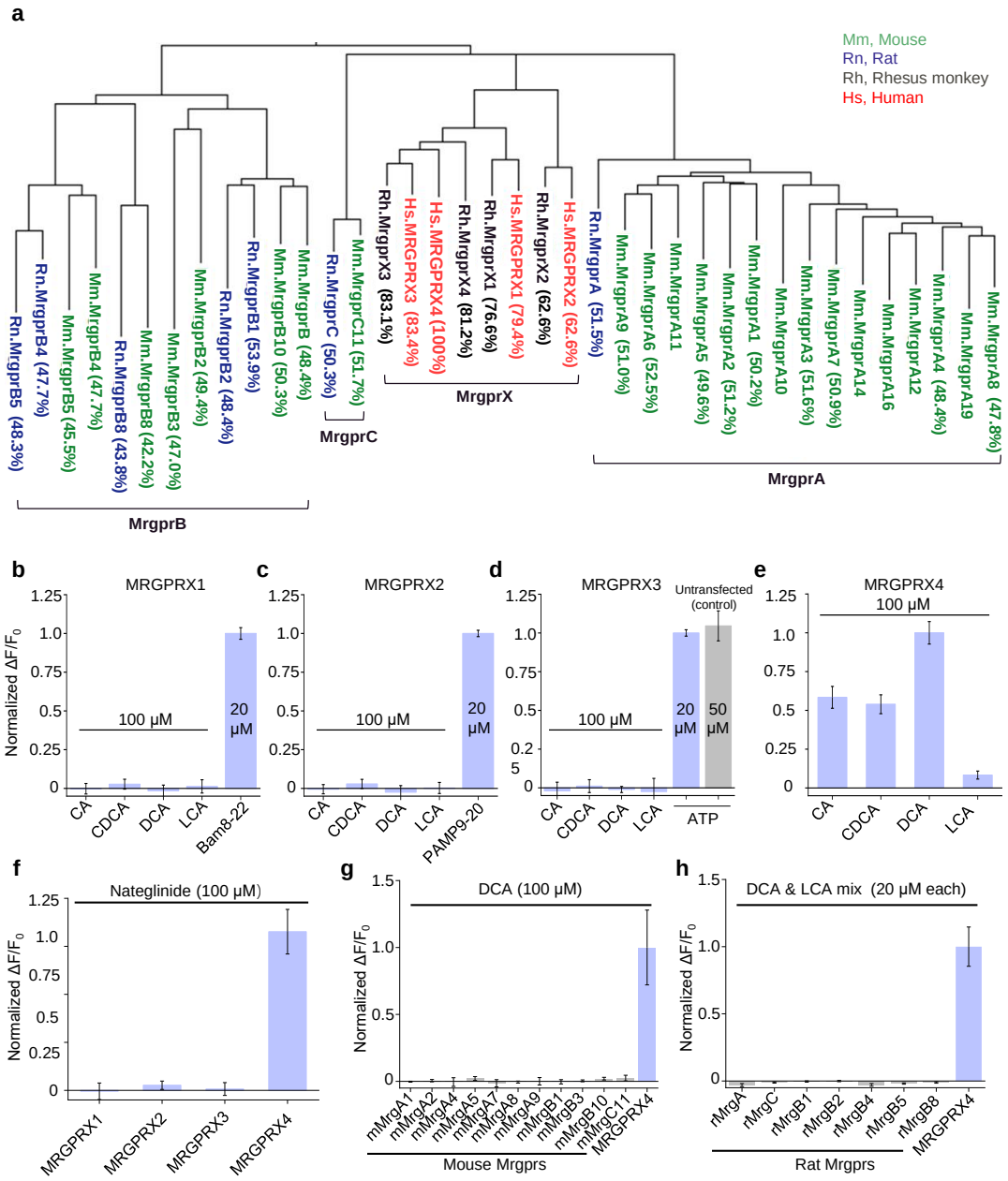

Supplementary Fig. 4 The anti-MRGPRX4 antibody has high specificity.

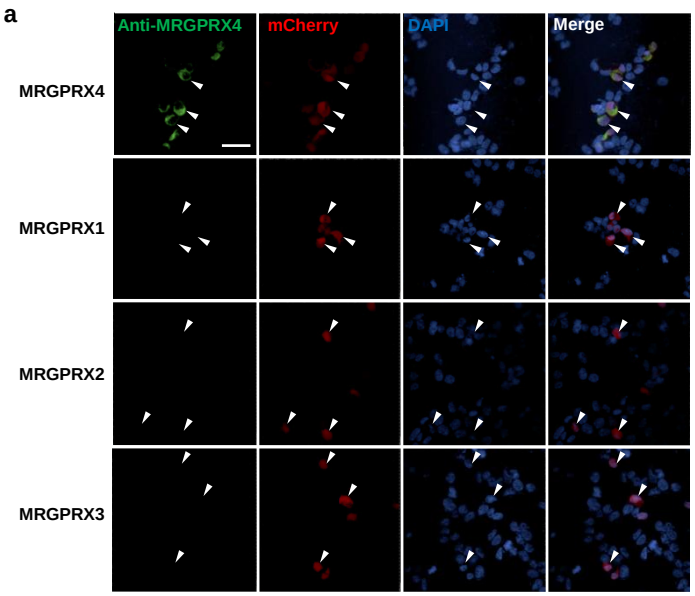

Supplementary Fig. S5. Expressing MRGPRX4 in cultured rat DRG neurons renders the cells responsive to bile acids.

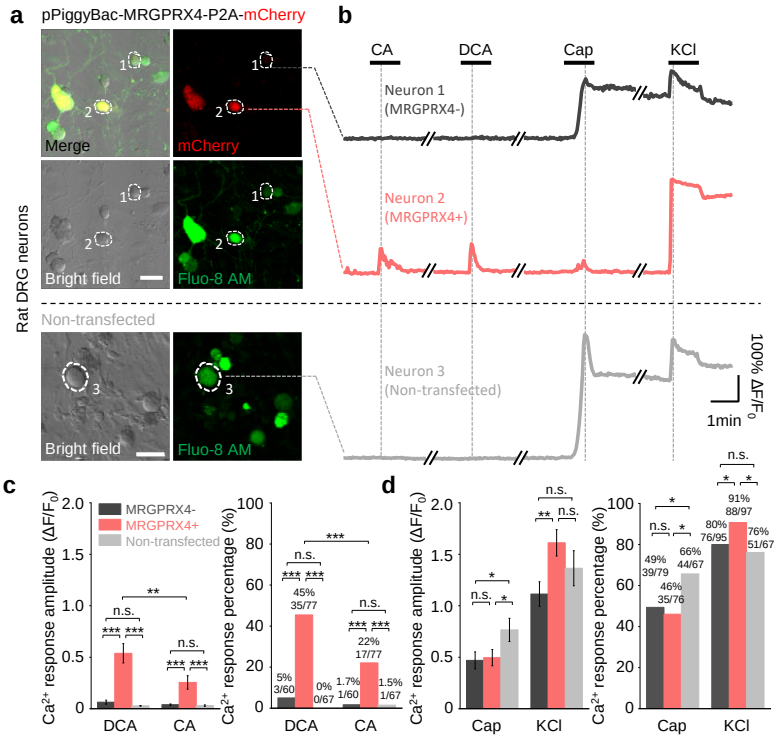

Supplementary Fig. 6 Cultured human DRG neurons respond to various chemicals

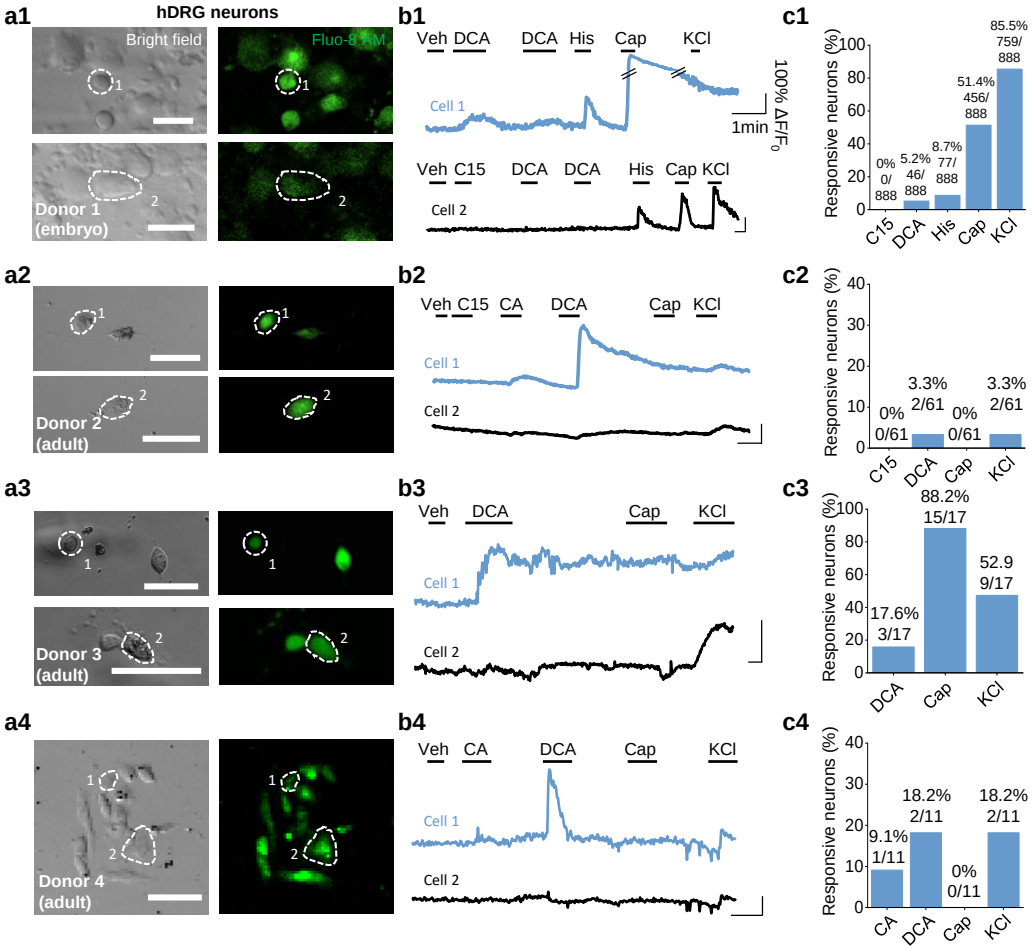

Supplementary Fig. 7 Expression of TGR5 in mouse and monkey DRG

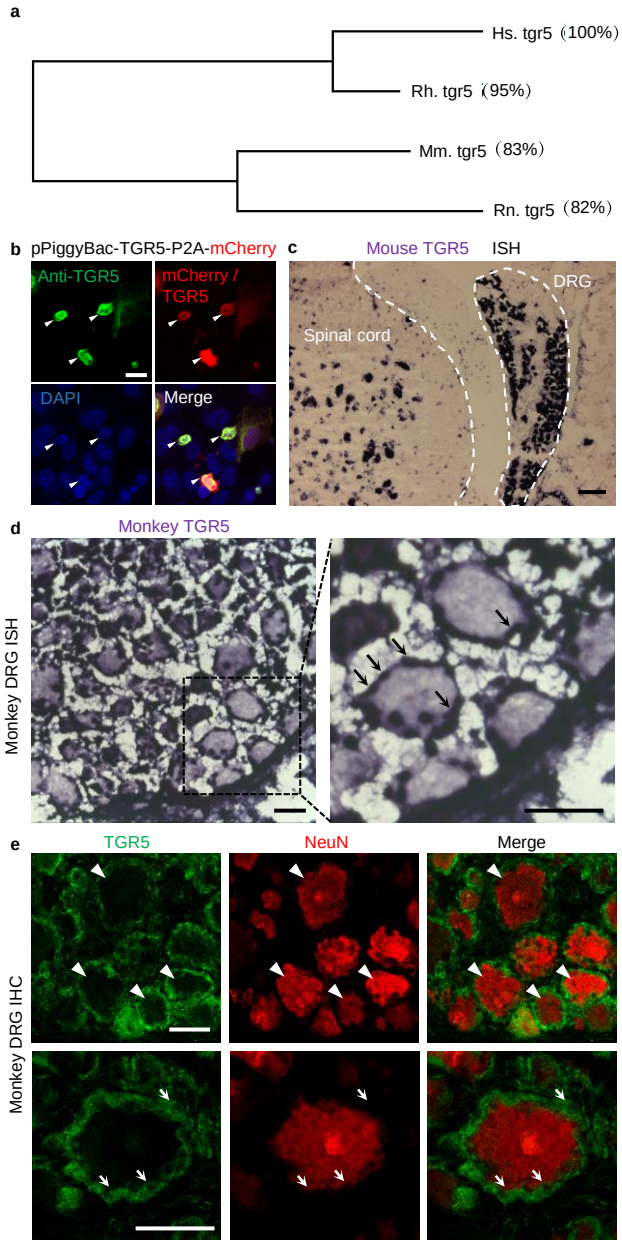

Supplementary Fig. 8 Quantification of bile acids in human plasma

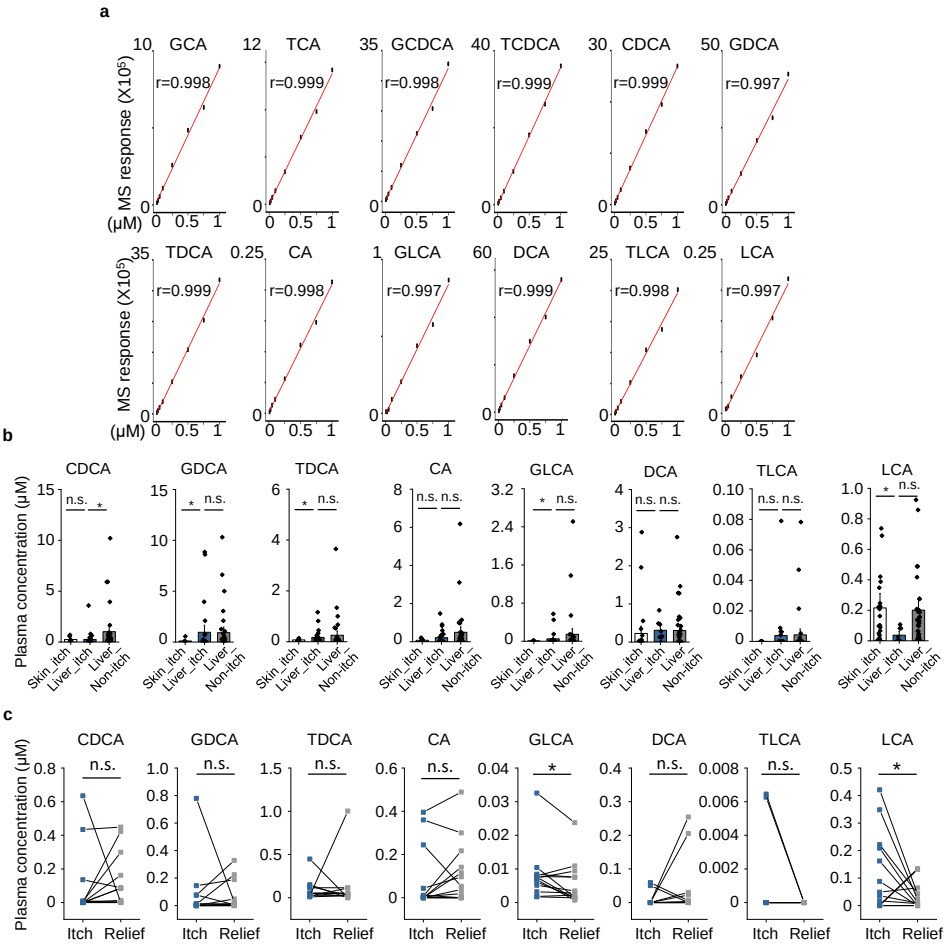

Supplementary Fig. 9 Bilirubin is an allosteric modulator and potentiates the activation of MRGPRX4 by bile acids and may contribute to cholestatic itch

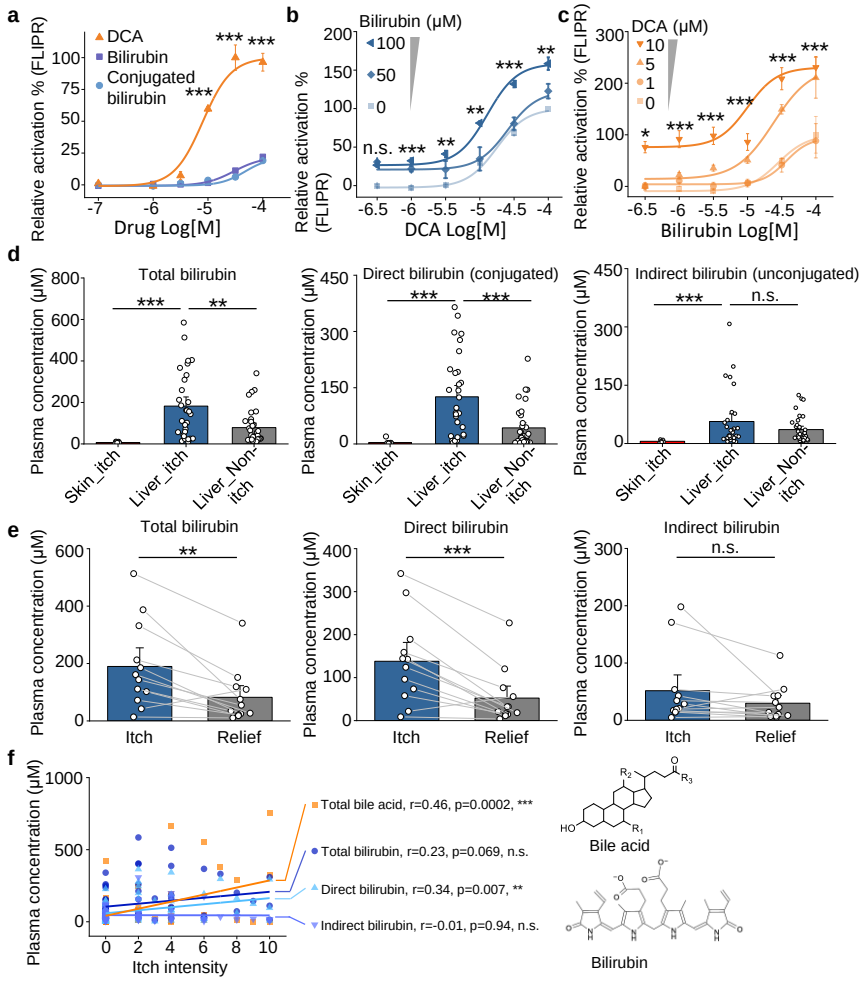

Supplementary Table 1 Genes that are highly expressed in human DRG

Rank	gene	DRG/All	Rank	gene	DRG/All	Rank	gene	DRG/All	Rank	gene	DRG/All	Rank	gene	DRG/All
1	LOC401164	1.0000	68	CCDC140	0.6985	135	ANKRD33	0.6209	202	GGT8P	0.5634	269	MAP7D2	0.5279
2	LOC645591	1.0000	69	PIRT	0.6964	136	CHRNA6	0.6181	203	CHRM4	0.5629	270	LOC100289511	0.5278
3	MIR1250	1.0000	70	VAT1L	0.6962	137	EPN3	0.6181	204	HOXC6	0.5627	271	SLC10A2	0.5276
4	MIR1914	1.0000	71	KRT75	0.6956	138	LIPM	0.6166	205	LOC100130298	0.5623	272	HSPA12A	0.5275
5	MIR3188	1.0000	72	HHLA1	0.6948	139	NBPF11	0.6150	206	LPAR3	0.5623	273	CYP4F24P	0.5273
6	MIR572	1.0000	73	RET	0.6899	140	KANK4	0.6145	207	FLJ42969	0.5611	274	RPL21P28	0.5260
7	MIR659	1.0000	74	GSX1	0.6867	141	OR13C5	0.6145	208	SLC2A6	0.5609	275	B4GALNT1	0.5253
8	MIR92B	1.0000	75	SCN10A	0.6867	142	SPDYE2	0.6136	209	FGF22	0.5606	276	CD1A	0.5253
9	MSGN1	1.0000	76	INSC	0.6863	143	PCDHAC2	0.6122	210	GRM4	0.5602	277	AATK	0.5249
10	OR10A4	1.0000	77	KCNK18	0.6858	144	PLD4	0.6120	211	FOXD3	0.5600	278	RXRG	0.5249
11	OR2M4	1.0000	78	OR2L13	0.6853	145	LOC100329108	0.6109	212	NKAIN4	0.5598	279	CRYBA2	0.5228
12	OR4H6P	1.0000	79	PRPH	0.6849	146	TRPV1	0.6099	213	LCNL1	0.5590	280	KCNA10	0.5221
13	OR56B2P	1.0000	80	LOC441617	0.6846	147	HOXD1	0.6098	214	TLX2	0.5588	281	SYT2	0.5214
14	P2RX6P	1.0000	81	SPTBN5	0.6845	148	OR56B4	0.6094	215	LOC100130275	0.5585	282	TSPAN10	0.5208
15	OR4N5	0.9985	82	SNORD123	0.6834	149	TLX3	0.6086	216	PDE6H	0.5579	283	SNORD116-21	0.5202
16	OR13C9	0.9799	83	CALCB	0.6819	150	PROKR2	0.6083	217	FOXS1	0.5576	284	INSRR	0.5201
17	SNORD87	0.9791	84	TMEM72	0.6789	151	KCNG4	0.6077	218	CHST8	0.5574	285	TUBB2A	0.5200
18	MIR324	0.9375	85	ADAMTS16	0.6761	152	NPSR1	0.6069	219	F2RL2	0.5564	286	C18orf42	0.5200
19	DYTN	0.9317	86	SNORA70B	0.6760	153	EGFL8	0.6065	220	MIR1247	0.5559	287	RESP18	0.5187
20	CRYGB	0.9233	87	MIR630	0.6754	154	FZD2	0.6061	221	GPR149	0.5547	288	PCDHAC1	0.5187
21	OR2M3	0.8983	88	SYT6	0.6753	155	SNORD125	0.6054	222	EMILIN3	0.5540	289	FLJ42875	0.5182
22	GPR139	0.8873	89	OR2T33	0.6725	156	TSHB	0.6045	223	TMEFF2	0.5527	290	OR2T32P	0.5177
23	MRGPRX4	0.8862	90	OTOP3	0.6707	157	KRT14	0.6042	224	HOXC4	0.5515	291	FCRLB	0.5170
24	SNORD91A	0.8861	91	BMP8B	0.6673	158	RASA4	0.6040	225	SLC3A1	0.5515	292	TMEM183B	0.5169
25	NOTO	0.8811	92	ISL2	0.6670	159	GLRA4	0.6034	226	MMD2	0.5508	293	THY1	0.5155
26	KRT32	0.8781	93	ENTPD2	0.6663	160	CHAT	0.6033	227	COL28A1	0.5498	294	FGF13	0.5154
27	NCRNA00052	0.8666	94	LOC644145	0.6660	161	C13orf36	0.6030	228	OR2W3	0.5496	295	LOC646329	0.5141
28	OR7E89P	0.8631	95	FAM19A3	0.6643	162	TTTY22	0.6019	229	PCSK2	0.5490	296	LOC100129726	0.5140
29	HCRT	0.8601	96	OR2T12	0.6639	163	POLR3G	0.6010	230	MIXL1	0.5477	297	SLITRK2	0.5140
30	MIR3907	0.8565	97	FGFBP3	0.6628	164	TTC24	0.6004	231	CADM3	0.5461	298	SHISA3	0.5138
31	OR2M1P	0.8519	98	TUSC5	0.6624	165	PRX	0.5978	232	BEAN1	0.5456	299	TMC3	0.5132
32	MRGPRX1	0.8291	99	CHRNA9	0.6583	166	LOC285401	0.5971	233	LOC645431	0.5454	300	P2RY12	0.5124
33	MRGPRD	0.8071	100	OTOF	0.6581	167	PLA2G3	0.5957	234	IMPDH1	0.5454	301	PRRG3	0.5114
34	NEFH	0.7988	101	ANGPTL7	0.6576	168	CCL1	0.5939	235	CLDN19	0.5443	302	MICALL2	0.5112
35	MRGPRE	0.7926	102	SHOX2	0.6566	169	KCND1	0.5920	236	LOC200726	0.5436	303	COL27A1	0.5110
36	P2RX3	0.7858	103	SLC18A3	0.6554	170	COL22A1	0.5899	237	FABP7	0.5431	304	SLC13A1	0.5108
37	PSMB11	0.7852	104	CALCA	0.6553	171	OR2L1P	0.5849	238	FAM90A10	0.5429	305	CHRNB3	0.5106
38	CST4	0.7728	105	PLEKHD1	0.6549	172	RDH12	0.5844	239	LOC440300	0.5426	306	FKBP1B	0.5104
39	HOXB8	0.7718	106	POU4F1	0.6519	173	FMO1	0.5841	240	MIA	0.5423	307	CCL3L3	0.5104
40	POU4F3	0.7700	107	NPPB	0.6511	174	NRG1	0.5841	241	PRG1	0.5421	308	PCBP3	0.5094
41	SNAR-B1	0.7700	108	IL31RA	0.6506	175	OR7E102P	0.5840	242	LRRC16B	0.5418	309	KCNA6	0.5091
42	SNAR-B2	0.7700	109	DEFB130	0.6499	176	LOC647012	0.5828	243	TRPV3	0.5412	310	GSTT2B	0.5084
43	FOSB	0.7584	110	LOC100133267	0.6499	177	AHNAK2	0.5827	244	VAMP1	0.5405	311	FXYD7	0.5083
44	LCTL	0.7571	111	SCN11A	0.6495	178	REEP1	0.5815	245	ISL1	0.5396	312	C2orf66	0.5082
45	TMEM132E	0.7539	112	GRIK3	0.6489	179	STMN2	0.5812	246	L1CAM	0.5396	313	OR7E59P	0.5080
46	BHLHA9	0.7505	113	FAM70A	0.6487	180	LOC100288346	0.5809	247	CHRFAM7A	0.5392	314	MOS	0.5076
47	SCGB1C1	0.7439	114	AMIGO3	0.6471	181	TSPAN11	0.5809	248	GPR83	0.5390	315	C17orf99	0.5076
48	NTRK1	0.7438	115	LOC574538	0.6467	182	CD1E	0.5802	249	LOC100129931	0.5388	316	PRSS35	0.5075
49	BARHL1	0.7424	116	OR7E130P	0.6463	183	PTPN20B	0.5801	250	AFAP1L2	0.5381	317	AURKB	0.5073
50	PRDM12	0.7422	117	TAC1	0.6449	184	HTR3A	0.5800	251	PDZD7	0.5377	318	LOC100130148	0.5067
51	FRMPD1	0.7377	118	BET3L	0.6440	185	NMB	0.5794	252	GNG3	0.5372	319	LRRTM1	0.5066
52	OR2T8	0.7376	119	SFRP4	0.6435	186	PCDH8	0.5786	253	GJC3	0.5371	320	HOXA6	0.5065
53	AVIL	0.7362	120	NEFM	0.6423	187	AQP12B	0.5781	254	CRYGD	0.5369	321	CYP1A1	0.5064
54	TRIM67	0.7359	121	POU4F2	0.6412	188	OR2A13P	0.5766	255	SNORD116-20	0.5365	322	PTPRN	0.5062
55	NBPF24	0.7344	122	MAST1	0.6374	189	HMX1	0.5754	256	RAB3D	0.5365	323	LOC100130954	0.5041
56	DRGX	0.7271	123	NGFR	0.6374	190	BTNL2	0.5754	257	CPEB1	0.5363	324	C17orf102	0.5039
57	TMEM179	0.7192	124	TUBB3	0.6367	191	ADIPOQ	0.5754	258	IFITM5	0.5358	325	C1orf130	0.5035
58	GFRA3	0.7188	125	KCNH6	0.6356	192	TMEM63C	0.5747	259	CYP2W1	0.5356	326	COL5A3	0.5035
59	NEFL	0.7183	126	VSTM5	0.6354	193	PRIMA1	0.5718	260	PODNL1	0.5344	327	FBXO2	0.5034
60	OR11H2	0.7176	127	MPZ	0.6344	194	OR7E163P	0.5713	261	KIF3C	0.5337	328	OR6B2	0.5022
61	CER1	0.7153	128	OR1H1P	0.6329	195	CHRNA7	0.5706	262	ADAMTSL1	0.5336	329	MATN2	0.5021
62	MIR570	0.7149	129	LOC149134	0.6309	196	EXTL1	0.5682	263	BCAN	0.5335	330	SLC17A6	0.5014
63	SHH	0.7125	130	AQP12A	0.6266	197	CLDN22	0.5679	264	DPYSL5	0.5313	331	CYSLTR2	0.5013
64	STAC	0.7121	131	KCTD8	0.6251	198	SCN4B	0.5672	265	HKDC1	0.5308	332	B4GALNT4	0.5008
65	MIR770	0.7100	132	TMEM233	0.6228	199	CPNE6	0.5667	266	CLEC2L	0.5298			
66	FLJ46446	0.7017	133	LOC284233	0.6224	200	SYNGR3	0.5663	267	DISP2	0.5288			
67	LOC727677	0.6995	134	TMPRSS5	0.6212	201	MIR339	0.5653	268	DHH	0.5286			

Supplementary Table 2 GPCRs expression profiling in human DRG

Rank	GPCR	DRG/All	Rank	GPCR	DRG/All	Rank	GPCR	DRG/All	Rank	GPCR	DRG/All	Rank	GPCR	DRG/All
1	**GPR139**	**0.887**	75	UTS2R	0.237	149	BAI2	0.132	223	GPRC5B	0.065	298	GPR39	0.017
2	**MRGPRX4**	**0.886**	76	HTR1B	0.235	150	HTR1F	0.131	224	GPR125	0.062	299	TSHR	0.015
3	**MRGPRX1**	**0.829**	77	CXCR3	0.235	151	P2RY11	0.131	225	ADRA2B	0.062	300	HCAR3	0.014
4	**MRGPRD**	**0.807**	78	OPRL1	0.233	152	ADORA1	0.131	226	F2R	0.060	301	RXFP1	0.012
5	**MRGPRE**	**0.793**	79	GABBR1	0.229	153	GPR45	0.129	227	GPR88	0.058	302	CHRM5	0.011
6	**PROKR2**	**0.608**	80	PTGER3	0.228	154	GPR12	0.129	228	GPR84	0.054	303	FFAR2	0.011
7	**NPSR1**	**0.607**	81	LPHN3	0.222	155	ADRA2C	0.128	229	GRM2	0.054	304	GPR182	0.010
8	**FZD2**	**0.606**	82	CELSR2	0.221	156	LPAR6	0.127	230	RHOD	0.054	305	CXCR1	0.009
9	**CHRM4**	**0.563**	83	GPR132	0.219	157	PTGER1	0.126	231	ADCYAP1R1	0.053	306	GPR97	0.008
10	**LPAR3**	**0.562**	84	GPR56	0.214	158	LPAR2	0.125	232	GPR22	0.052	307	CXCR2	0.007
11	**GRM4**	**0.560**	85	PTGER2	0.214	159	ADRB2	0.123	233	GPR135	0.052	308	F2RL3	0.006
12	**F2RL2**	**0.556**	86	GPR61	0.210	160	HTR4	0.123	234	CHRM3	0.050	309	NTSR1	0.005
13	**GPR149**	**0.555**	87	GPR64	0.209	161	ADORA2B	0.122	235	FPR1	0.050	310	GRM3	0.004
14	**GPR83**	**0.539**	88	BDKRB2	0.209	162	GPR75	0.119	236	SSTR3	0.050	311	GRM5	0.004
15	**P2RY12**	**0.512**	89	GPR142	0.208	163	TGR5	0.117	237	GPR15	0.050	312	S1PR5	0.002
16	**CYSLTR2**	**0.501**	90	P2RY1	0.207	164	CRCP	0.116	238	S1PR4	0.049	313	ADRB3	0.000
17	HTR1D	0.489	91	GPR98	0.204	165	GPR176	0.114	239	LPHN2	0.049	314	AGTR2	0.000
18	GPR114	0.487	92	PTGER4	0.199	166	NMUR1	0.114	240	OXTR	0.049	315	AVPR1B	0.000
19	GPR173	0.482	93	GPR152	0.196	167	MCHR1	0.114	241	FZD9	0.048	316	BRS3	0.000
20	CCKAR	0.478	94	HCAR1	0.194	168	GNRHR	0.112	242	GPR52	0.047	317	CCR3	0.000
21	MC5R	0.461	95	LTB4R	0.192	169	S1PR2	0.111	243	GPR55	0.047	318	CCR7	0.000
22	OPRK1	0.457	96	LPHN1	0.192	170	GPR183	0.110	244	GPR113	0.047	319	CCR8	0.000
23	GPR35	0.457	97	GPR133	0.191	171	HTR6	0.110	245	CCRL2	0.046	320	CNR2	0.000
24	FFAR1	0.447	98	P2RY6	0.188	172	FZD6	0.107	246	GPR179	0.046	321	DRD3	0.000
25	CX3CR1	0.445	99	GNRHR2	0.187	173	ADORA2A	0.104	247	ADRA1B	0.045	322	FPR2	0.000
26	FZD8	0.441	100	GPR34	0.187	174	GPR25	0.102	248	CELSR1	0.044	323	GALR3	0.000
27	GPR27	0.440	101	GPR126	0.185	175	P2RY2	0.102	249	APLNR	0.044	324	GHRHR	0.000
28	LGR5	0.436	102	RXFP3	0.184	176	GPR65	0.102	250	GRM6	0.043	325	GHSR	0.000
29	QRFPR	0.434	103	NPY5R	0.184	177	GPRC5C	0.101	251	GPR160	0.043	326	GPR101	0.000
30	GPR128	0.426	104	HTR5A	0.179	178	C5AR1	0.098	252	GIPR	0.043	327	GPR110	0.000
31	LHCGR	0.425	105	GPR153	0.179	179	FZD3	0.098	253	GPR116	0.043	328	GPR112	0.000
32	OPRD1	0.416	106	CXCR4	0.179	180	PTGIR	0.097	254	GPR141	0.043	329	GPR119	0.000
33	PTGFR	0.405	107	GPR19	0.179	181	P2RY8	0.096	255	HTR1E	0.043	330	GPR144	0.000
34	MRGPRX3	0.379	108	CRHR1	0.177	182	GPR174	0.095	256	GPR62	0.043	331	GPR148	0.000
35	MAS1L	0.378	109	CCR2	0.174	183	PTH2R	0.094	257	CCR4	0.041	332	GPR150	0.000
36	NPFFR2	0.377	110	GPR17	0.173	184	GPR3	0.093	258	NMUR2	0.041	333	GPR151	0.000
37	GPR37L1	0.373	111	GPR50	0.173	185	GPR26	0.092	259	HTR2A	0.040	334	GPR31	0.000
38	DRD2	0.368	112	CASR	0.172	186	GRM8	0.092	260	GPR123	0.039	335	GPR32	0.000
39	GPR161	0.360	113	TBXA2R	0.170	187	EMR4P	0.091	261	CHRM1	0.039	336	GPR6	0.000
40	PTGDR	0.350	114	HRH4	0.167	188	NMBR	0.090	262	GPR4	0.038	337	GPR78	0.000
41	P2RY14	0.335	115	CCR6	0.167	189	CXCR6	0.089	263	GPR21	0.037	338	GPR87	0.000
42	NPFFR1	0.329	116	AVPR2	0.167	190	TAS1R3	0.088	264	PPYR1	0.037	339	GPRC5D	0.000
43	GRM7	0.326	117	CYSLTR1	0.166	191	CCR5	0.088	265	ELTD1	0.036	340	GPRC6A	0.000
44	HRH1	0.320	118	GPR115	0.165	192	GPR77	0.087	266	EMR1	0.036	341	HCRTR1	0.000
45	CRHR2	0.317	119	CALCR	0.161	193	FZD4	0.087	267	FZD5	0.033	342	HTR1A	0.000
46	FZD1	0.313	120	GPR68	0.159	194	SSBP1	0.086	268	LTB4R2	0.033	343	KISS1R	0.000
47	SSTR4	0.311	121	TRIM5	0.158	195	CCRL1	0.085	269	HCAR2	0.032	344	LPAR4	0.000
48	GPR124	0.305	122	TACR1	0.157	196	DRD1	0.085	270	CALCRL	0.032	345	MC2R	0.000
49	BAI1	0.304	123	O3FAR1	0.157	197	MC4R	0.083	271	F2RL1	0.032	346	MC3R	0.000
50	CCR10	0.304	124	CCKBR	0.156	198	SSTR2	0.082	272	AVPR1A	0.031	347	MCHR2	0.000
51	LPAR5	0.298	125	HRH3	0.156	199	GPR162	0.082	273	GPR37	0.028	348	MLNR	0.000
52	LPAR1	0.294	126	GLP1R	0.156	200	MTNR1A	0.081	274	S1PR1	0.028	349	MRGPRG	0.000
53	DRD4	0.293	127	GPR82	0.155	201	CCBP2	0.080	275	TACR2	0.028	350	MRGPRX2	0.000
54	PROKR1	0.291	128	GPR20	0.155	202	CCR1	0.080	276	SUCNR1	0.027	351	MTNR1B	0.000
55	BAI3	0.288	129	CMKLR1	0.154	203	HRH2	0.079	277	GPR1	0.026	352	NPBWR1	0.000
56	ADRA1D	0.287	130	CXCR7	0.151	204	BDKRB1	0.078	278	CHRM2	0.025	353	NPBWR2	0.000
57	GALR1	0.285	131	C3AR1	0.150	205	DARC	0.077	279	GRM1	0.025	354	NPY2R	0.000
58	FZD7	0.282	132	S1PR3	0.149	206	GPR111	0.076	280	HTR2C	0.025	355	OPN5	0.000
59	GPR156	0.281	133	GPR85	0.147	207	ADORA3	0.075	281	LGR6	0.024	356	P2RY10	0.000
60	P2RY13	0.274	134	PTAFR	0.147	208	OXGR1	0.073	282	EMR3	0.024	357	PRLHR	0.000
61	CCR9	0.273	135	Tpra1	0.147	209	GRPR	0.072	283	GPR18	0.024	358	RXFP2	0.000
62	SMO	0.270	136	NPY1R	0.144	210	MRGPRF	0.072	284	GLP2R	0.024	359	RXFP4	0.000
63	P2RY4	0.266	137	OXER1	0.143	211	HCRTR2	0.071	285	AGTR1	0.024	360	SSTR5	0.000
64	GABBR2	0.262	138	OPN3	0.143	212	CNR1	0.070	286	FSHR	0.023	361	TAAR3	0.000
65	FZD10	0.260	139	Gpr137	0.142	213	MAS1	0.070	287	Gpr143	0.023	362	TAAR5	0.000
66	EDNRB	0.259	140	EDNRA	0.140	214	OPRM1	0.070	288	ADRB1	0.023	363	TAAR6	0.000
67	MC1R	0.258	141	GPR157	0.140	215	C17orf103	0.070	289	VIPR1	0.023	364	TAAR8	0.000
68	CELSR3	0.257	142	GPR146	0.139	216	CD97	0.070	290	VIPR2	0.022	365	TACR3	0.000
69	ADRA2A	0.252	143	GPER	0.137	217	NTSR2	0.067	291	HTR2B	0.021	366	TAS1R2	0.000
70	DRD5	0.249	144	GPR63	0.136	218	FFAR3	0.066	292	CXCR5	0.020	367	TRHR	0.000
71	LGR4	0.242	145	TAS1R1	0.134	219	SCTR	0.066	293	ADRA1A	0.019	368	XCR1	0.000
72	HTR7	0.241	146	NPY6R	0.134	220	SSTR1	0.066	294	GPRC5A	0.018			
73	GPR158	0.240	147	PTH1R	0.134	221	EMR2	0.066	295	GALR2	0.018			
74	Gpr107	0.240	148	FPR3	0.133	222	GCGR	0.065	296	GPR171	0.017			